2020

ACETOACETATE ENHANCES OXIDATIVE METABOLISM AND RESPONSE TO TOXICANTS OF CULTURED RENAL CELLS

Trudi Maria Denoon

ACETOACETATE ENHANCES OXIDATIVE METABOLISM AND RESPONSE to TOXICANTS of CULTURED RENAL CELLS

A dissertation submitted in partial fulfillment

Of the requirement for the degree of

DOCTOR OF PHILOSPHY

To the faculty of the

DEPARTMENT OF PHARMACEUTICAL SCIENCES

COLLEGE OF PHARMACY AND HEALTH SCIENCES

at

ST. JOHN'S UNIVERSITY

New York

by

TRUDI M. DENOON

Date Submitted: _____ Date Approved: _____

_____ _____

Trudi M. Denoon Dr. Sue M. Ford

ABSTRACT

ACETOACETATE ENHANCES OXIDATIVE METABOLISM AND RESPONSE to TOXICANTS of CULTURED RENAL CELLS

Trudi Denoon

In vitro methods can be cost effective and facilitate large scale drug screening in the pharmaceutical industry. Renal proximal tubular cells have been a prime target for drug induced toxicity. LLC-PK_1 cells possess many transport functions of the proximal tubule epithelia, however, its energy metabolism differs from the highly oxidative tubule metabolism in vivo. This may impact its reliability in predicting toxicity. Modulating the growth media composition has been shown to shift cultured liver and muscle cells from high glycolytic activity to increased oxidative metabolism, but few studies have been done on renal cells.

This study is designed to test the impact of growth media modulation on mitochondrial respiration and glycolytic activity of LLC-PK_1 cells via measurement of oxygen consumption rate (OCR) and extracellular acidification rate (ECAR) using the Seahorse XFp Analyzer (Agilent Technologies). Cells were grown to confluence in SFFD (50:50 DMEM-Ham's nutrient mix F-12 with 15 mM HEPES) culture medium containing 3% FBS and 5mM glucose or 5mM glucose supplemented with 5mM acetoacetate. Extracellular flux (XF) analysis showed that the basal respiration, maximal respiration, spare respiratory capacity and ATP-linked respiration were significantly increased, indicating an increase in mitochondrial function. The increase in mitochondrial function was accompanied by an increased expression in biomarkers

of mitochondrial biogenesis, PGC-1α and TFAM. There was also an increase in mitochondrial COX IV expression. Additionally, XF analysis also showed a significant decrease in glycolytic capacity and reserve for the acetoacetate group.

LC_{50} values for mitochondrial toxicants, clotrimazole, diclofenac and ciprofibrate were assessed via a modified trypan blue staining assay. Cells grown in media complemented with acetoacetate displayed significantly lower LC_{50} values when treated with clotrimazole and diclofenac. There was a marked increase in uncoupled respiration in the presence of diclofenac, while clotrimazole and ciprofibrate significantly decreased respiration in the acetoacetate group. In conclusion, acetoacetate complemented media can alter the cellular metabolism of the LLC-PK_1 cell line and increase its sensitization to toxicants, thus making this a better model for toxicity drug screening.

ACKNOWLEDGEMENTS

I would like to sincerely thank Dr. Sue M. Ford for her guidance, tutelage, and knowledge. I am grateful for having been her student and having the privilege to grow and develop as a scientist under her mentorship. I am also indebted to Dr. V. Korlipara, Chairman of the Department of Pharmaceutical Studies, who provided me with the tools and skills to successfully complete this project.

I would also like to extend this gratitude to Dr. Joanne Carroll, Dr. Raymond Ochs, Dr. Frank Schanne, and Dr. Louis Trombetta for being members of my committee. Their support, wisdom, and professional guidance have made a profound impact on the completion of this project. Genuine gratitude is extended to the Pharmaceutical Sciences Department and by extension St. John's University for providing the financial support and opportunity to serve as both a Graduate Assistant and Teaching Fellow during my tenure at St. John’s University.

I am also grateful for lab mates and colleagues, past and present. I am humbled by the unending support of my friends Belkys, and Siddharth who were there to offer advice and provide clarity. I would also like to include Benjamin and Olivia who were always there to lend a hand whenever it was needed.

My family has been the source of my motivation that was necessary to complete this journey. I am forever indebted to them for their unconditional love, support and sacrifices that allowed me to pursue my dreams. Finally, this is dedicated to the memory of my aunts May Denoon and Alice Francis. Their love and support were instrumental in my achievements. They were a source of light on many dark days.

TABLE OF CONTENTS

LIST OF TABLES

LIST OF FIGURES

1. INTRODUCTION

The drug development process can consist of three parts namely, drug discovery, preclinical development and clinical trial (Steinmetz and Spack 2009). Pre-clinical research is an important step in the drug development process. It is necessary for researchers to assess potential new drugs for toxicity before progressing to the clinical research phase of the new development process. Preclinical studies will assess efficacy, explore pharmacology and utilize toxicology-based assays that establish dose, route and frequency that will be used in subsequent studies (Steinmetz and Spack 2009). The studies are usually designed to assess absorption, distribution, metabolism and excretion (ADME) and bioavailability parameters of the new drug (Steinmetz and Spack 2009). For this reason, current pre-clinical development is dependent on *in vitro* and *in vivo* studies.

Pharmaceutical xenobiotics intended to be therapeutics can have deleterious effects on mitochondrial function (Will and Dykens 2014). Most of these side effects, such as electron transport chain (ETC) inhibition and uncoupling of ATP production are not always detected by the preclinical cell-based and animal studies (Will and Dykens 2014). Toxicity often remains undetected until large numbers of patients have been exposed (Will and Dykens 2007). Mitochondrial impairment typically affects the most aerobically poised tissues, such as kidney and heart, or tissues exposed to higher concentrations of the drug, such as the liver (Will and Dykens 2007). Pharmaceuticals such as cerivastatin, have been withdrawn from the market due to adverse effects on the kidney and heart (Will and Dykens 2007).

A major disadvantage of currently used immortalized *in vitro* models is that they are less sensitive than primary renal tubular cells to nephrotoxicants (Li et al. 2013). Primary cells in culture can be used for toxicity testing given their metabolic activity (Marroquin et al. 2007). Yet the difficulties with isolation and brief survival rate can increase the cost of maintenance and limit their utility. Although immortalized cell lines are cheaper alternatives, studies have highlighted that most drugs fail at the clinical testing phase due to poor predictability during *in vitro* testing (Li et al. 2013). A study designed to evaluate the Environmental Protection Agency (EPA) ToxCast catalog of chemicals, conducted a high-throughput screening assay of compounds with mitochondrial liabilities (Wills et al. 2015). Rabbit primary renal proximal tubular cell (RPTC) and was exposed to 676 compounds from the ToxCast catalog. RPTC identified 486 of these compounds as ETC inhibitors. A third of these compounds (131) were exposed to the immortal cell line human kidney 2 (HK2). This cell line only identified 14 compounds as ETC inhibitors (Wills et al. 2015). This indicates that there is a reduced sensitivity and low predictability in immortal renal cell lines.

A possible solution would require the use of cells lines that have improved sensitivity, eliminating some of the pitfalls that commonly plague cells in culture. Immortalized and/or tumor derived cell lines are adapted to grow rapidly under hypoxic and acidic conditions as they meet their energy requirements via glycolysis (Marroquin et al. 2007). These cells are usually cultured in high glucose concentration such as 25 mM resulting in the Crabtree effect, which is the glucose induced inhibition of oxidative phosphorylation due to the inhibitory effects of

fructose 1,6 bisphosphate (Marroquin et al. 2007). There is glucose induced stimulation of hexokinase and phosphofructokinase-1 activity, resulting in an increase in fructose 1,6 bisphosphate (Rodriguez-Enriquez et al. 2001). Fructose 1,6 bisphosphate can activate pyruvate kinase, which irreversibly catalyzes the second glycolytic reaction that generates ATP (Marroquin et al. 2007). Thus, there is an overall increase in the glycolytic flux with a concomitant decrease in oxidative metabolism as pyruvate the terminal product in glycolysis, is converted to lactate. Under these conditions, most cells derive most of their ATP from glycolysis, not from oxidative phosphorylation (Will and Dykens 2014). Cells cultured in this manner will be less sensitive to mitochondrial toxicants and limit their utility as predictors of adverse effects and toxicity of mitochondrial drug/compounds (Marroquin et al. 2007).

The human immortalized cell lines that do not accurately report mitochondrial liabilities can result in huge costs to the pharmaceutical industry with hepatoxic, cardiotoxic and nephrotoxic effects. Kidneys are organs that are susceptible to mitochondrial toxicants, due to drug metabolism (biotransformation) and high energy demand. Kidney cell lines such as human kidney cell line 2 (HK-2) have high rates of glycolytic activity and do not accurately screen for mitochondrial toxicants (Wills et al. 2015). Altering growth media composition with different substrates has been shown to shift cultured liver and muscle cells from high glycolytic activity to increased oxidative metabolism, but few studies have been done on renal cells. Thus, media modulation might reprogram the cell lines routinely used in toxicity testing and can improve their usefulness in high throughput screening.

Kidney structure, function and metabolism

The kidneys regulate body fluid volume, secrete hormones, and excrete waste products and xenobiotics (Stallons et al. 2013). Renal epithelial cells meet most of their energy demands through oxidative metabolism and are susceptible to injury from mitochondrial toxicants (Stallons et al. 2013). Ninety percent of drug induced kidney injury takes place within the proximal tubule due to their elevated metabolic activity, increased number of transporters, higher blood flow and greater oxygen tensions (Bonventre et al. 2010).

Blood plasma is filtered by the glomerulus and moves into the proximal tubule. The processing of the filtrate helps to eliminate waste while regulating fluid, electrolyte and acid-base balance (Bonventre et al. 2010). The proximal tubular cells are sensitive to drug induced toxicity due to its role in concentrating the glomerular filtrate. Nephrotoxicants in the filtrate can be concentrated fivefold in the proximal tubules (Bonventre et al 2010). Most xenobiotics are removed from circulation via transporter-mediated secretion which primarily occurs in the proximal tubules (George et al. 2017).

Transporters that line the tubules are necessary for the regulation of the fluid and utilize substantial amounts of energy. As a result, the proximal tubules are rich in mitochondria and meet their energy demands via oxidative phosphorylation (Norbakhsh and Singh, 2014). A major task of proximal tubular cells is the active transport of sodium, which maintains the driving force for the coupled reabsorption of

solutes and water (Gstraunthaler et al. 1999). Approximately 80% of oxygen consumed for ATP production supports active sodium transport, while 15-20% accounts for basal metabolic activity (Nourbakhsh and Singh, 2014). In the kidney, the rate of respiration linearly follows the rate of active transport (Mandel 1986). About 70% of proximal tubular cell oxygen consumption is metabolically used to fuel Na+/K+-ATPase activity (Gstraunthaler et al. 1999). Increase in Na+/K+-ATPase activity increases the demand for ATP, resulting in an increase in respiration (Mandel 1986).

Oxidative phosphorylation is an energy pathway that can provide enough ATP to support the rate of active transport in the kidney. Oxidative phosphorylation can yield 38 molecules of ATP from one molecule of glucose whereas glycolysis can yield 2 net molecules of ATP from one molecule of glucose (Nourbakhsh and Singh, 2014). Therefore, oxidative metabolism can meet the energy demands of the kidney. These chemicals are then cleared from the tubular cells by transporters on the apical/tubular membrane and added to the filtrate (George et al. 2017).

However, some compounds are reabsorbed by the apical transporters which increases the net intracellular concentrations of drugs and xenobiotics resulting in deleterious effects. Additionally, basolateral uptake from the peritubular capillaries can also increase the intracellular concentrations of toxicants (Bonventre et al. 2010). The excretion of the herbicide paraquat provides a demonstrable example of transport induced tubular injury. The kidneys are responsible for eliminating the majority of paraquat is absorbed into systemic circulation (George at al. 2017). *In vitro* transport studies in LLC-PK_1 cells have indicated that the basolateral transporter, organic

cation transporter 2 (OCT2), mediated the uptake of paraquat from the blood and is responsible for its intracellular accumulation (George et al. 2017). Paraquat participates in redox cycling that produces in superoxide formation, resulting in tubular degeneration and necrosis (George et al. 2017)

The tubules contain drug metabolizing enzymes that participate in biotransformation, which can potentiate the toxicity to tubular cells (Bonventre et al. 2010). Cytochrome P450 enzymes and the enzymes of conjugation are found mainly in the cortex, the location for the proximal tubule (Lohr et al. 1998). The drug metabolizing enzymes alter the parent compounds, making them more polar. This facilitates excretion (Lohr et al. 1998). Amino acid conjugation results in loss of pharmacological activity for some compounds. This increases the probability of excretion via tubular secretion methods (Lohr et al. 1998).

Glycine conjugation increases the polarity of benzoic and salicylic acid which facilitates their excretion (Lohr et al. 1998).

Biotransformation can result in conversion of parent compounds to toxic metabolites that can accumulate in the intracellular regions of the tubular cells. The high mitochondrial density cells that line the tubules, make proximal tubular cells and by extension the kidney susceptible to mitochondrial toxicants (Lohr et al. 1998). Beta lactam antibiotics such as cephaloridine, were shown to accumulate in rat proximal tubular cells via interaction with the apical basolateral organic anion transporter 3 (OAT 3) (George et al. 2017).

An in depth look at energy metabolism in the kidney, indicates that glucose is not the preferred energy substrate. The oxidation of long-chain fatty acids has been

taken to contribute 50-80% of the fuel of respiration of the kidney (Weidemann and Krebs 1969). In cortical slices of male rats, 5 mM glucose contributed 30.3% to the respiratory fuel and only 11.3% after starvation (Weidemann and Krebs 1969). Acetoacetate (5 mM) or butyrate (10 mM) provided up to 80%, in comparison to oleate (2 mM) which provided up to 50% of the fuel of respiration in male rate cortical slices (Weidemann and Krebs 1969). Therefore, glucose provided the lowest contribution the respiratory fuel, suggesting that it is not the preferred substrate *in vivo*. Fatty acid and ketone body metabolism takes place in the mitochondria. Given the high mitochondrial density of the proximal tubular cells, the above-mentioned substrates are better sources of energy for the kidney.

Thus, the kidney is an organ that is extremely sensitive to toxicants. However, its *in vitro* counterparts do not reflect the *in vivo* findings. Current pre-clinical *in vitro* toxicity contributes to drug attrition during pre-clinical studies and phase 3 (Li et al. 2013). Models used in pre-clinical testing have low predictability due to the reduced sensitivity resulting in the late detection of renal toxicity. One reason there is decreased sensitivity is the increased dependence on glycolysis to meet energy demands. (Wills et al. 2015). Thus, there is a need for an improved model that reflects the activity often seen *in vivo.*

In vitro models: toxicity screening

Current methods in pre-clinical development utilize both *in vitro* and *in vivo* testing platforms (Steinmetz and Spack, 2009). However, there is the desire to reduce animal testing and improve the reliability of *in vitro* toxicity testing. *In vitro* cell

culture systems are a cost-effective method that facilitates drug toxicity identification in organ systems (Li et al. 2003). *In vitro* models can facilitate the identification of mechanisms of drug induced toxicity that are often complicated by multi organ systems present in the in vivo model (Davila et al. 1998). It has been shown that many drugs target renal proximal tubular cells. These cells are sensitive to many chemical agents and serves as a prime target for drug induced toxicity. (Li et al. 2003). Renal proximal tubular cells are responsible for excreting many metabolites, xenobiotics and drugs (Li et al. 2003). Thus, continuous cell lines as well as primary cultures are powerful tools for studying the biochemical and physiological characteristics of renal proximal tubular cells (Gstraunthaler et al. 1999). Renal tubular cells isolated from humans and animals can be used successfully to assess the physiological roles of the kidney (Li et al. 2003).

Human primary cells are difficult to obtain in substantial amounts and even more difficult to maintain. As a result, continuous or immortal cell lines can be a suitable alternative. The human kidney cell line 2 (HK-2), and the human embryonic kidney 293 (HEK293, HEK-293, or HEK) cells are human proximal tubular cell lines that are routinely used for *in vitro* toxicity testing. Current human kidney cell lines have been transfected with viral genes to make them immortal (Heussner and Dietrich 2013). HK-2 cells have been transfected with HPV virus, while the HEK 293 cells have been transfected with the adenovirus 5 (Heussner and Dietrich 2013). Additionally, immortalized cell lines are metabolically adapted for rapid growth and they derive almost all their energy from glycolysis (Marroquin et al. 2007). These

cells are typically grown in 25 mM glucose (450 mg/dL), fivefold higher than the physiological level (90 mg/dL) (Marroquin et al. 2007).

An article published by Lauren Willis and co-workers in April 2015, demonstrated that immortalized cell lines may not fully detect mitochondrial toxicants. 19 compounds were identified as cytotoxicants in rabbit primary renal proximal tubular cells (RPTC). However, 15 had no effect on viability in HK-2 cells (Wills et al. 2015). HK-2 cells are cultured in Roswell Park Memorial Institute 1640 Medium (RPMI) and consists of 10 mM glucose and 10 % FBS (Wills et al. 2015). Additionally, HK-2 cells do demonstrate dome formation, a hallmark of active sodium transport and an important feature of proximal tubular cells.

Porcine kidney cells can be used as an alternative to human cell lines. The porcine kidney shares anatomical and physiological features with that of human kidney and is relatively accessible (Heussner and Dietrich 2013). Fully sequenced porcine transporters (Oat1 and 3) demonstrate higher structural/amino acid identity to the human homologues when compared to those of either mice or rats. (Heussner and Dietrich 2013). Therefore, a porcine renal *in vitro* model can be a cheaper model that is easier to maintain than its human counterparts.

The LLC PK-$_1$ cells are derived from the Hampshire pig (Lohr et al. 1998). The LLC PK-$_1$ cell line has been one of the most characterized lines that has not been malignantly transformed unlike the HK-2 and HEK 293 cells. It is an established cell line derived from porcine cells of a Hampshire male pig and was successfully

developed by the Eli Lilly Company. Hull and co-workers indicated that LLC-PK_1 cells retain many properties and functions that are characteristic of tubular cells belonging to normal porcine kidneys. LLC-PK_1 cells have retained characteristic in vivo ion and solute transport (sodium transport and activity of Na, K-ATPase) as evidenced by dome formation (Felder et al. 2002). Domes are formed by cells that detach themselves from the substratum, owing to the buildup of pressure on the basolateral side of the monolayer due to transepithelial transport of salt and water and the potency of the tight junctions in making the monolayer impermeable to fluid. This dome formation results from the monolayer formed by the cells in culture (Hull et al. 1976).

Although cultured renal porcine proximal tubule cells maintain many of their in vivo characteristics, it has been demonstrated that these cells dedifferentiate from an oxidative metabolism to high rates of glycolysis. This is highly uncharacteristic of proximal tubular cells and is typically not seen *in vivo* (Felder et al. 2002). The most prominent observable changes are the decline in enzymes associated with oxidative metabolism coupled with an increase in glycolysis (Gstraunthaler et al. 1999). LLC-PK_1 cells demonstrated a decline in apical microvilli and mitochondrial volume. These changes were accompanied by an increase in glycolytic enzymes such as hexokinase (HK), phosphofructokinase (PFK), pyruvate kinase (PK) and lactate dehydrogenase (LDH) (Gstraunthaler et al. 1999).

There are several reasons that can contribute to this observable characteristic. Reduced oxygenation of the cultured cells has been indicated as one reason for the decline oxidative metabolism (Felder et al. 2002). Some studies have utilized media

supplementation and shaking media culture conditions to increase oxygen supply and improve oxidative metabolism in RPTC (Nowak and Schnellman 1995). In Gstraunthaler et al. (1999), a roller bottle method was utilized to improve oxygenation of epithelial monolayers. LLC-PK_1 cells were cultured in Dulbecco's Modified Eagle's Medium (DMEM) with low glucose (5.5 mM), and grown on the wall of cylindrical bottle that turned at 60 rev/hr. The combination of low glucose and increased oxygenation significantly decreased expression of glycolytic enzymes HK, PFK and LDH (Gsthraunthaler et al. 1999).

Immortalized and/or tumor derived cell lines are adapted to grow rapidly and exhibit abnormal energy metabolism when they are grown in standard cell culture conditions in the presence of media containing high concentrations of glucose (Nowak and Schnellman 1995). High glucose concentrations such as 25mM can induce the Crabtree effect, which is the glucose mediated inhibition of oxidative phosphorylation (Diaz-Ruiz et al. 2008). Phosphofructokinase (PFK), a regulatory enzyme for glycolysis, showed a steady increase in activity in LLC-PK1 when glucose concentrations increased from 1.85 to 5.5 mM (Gstraunthaler et al. 1999). This indicates that increasing concentrations of glucose will stimulate glycolytic activity.

The Crabtree effect is described as a reversible switch between glycolysis and oxidative metabolism that is dependent on the presence of glucose (Diaz-Ruiz et al. 2008). This differs from the Warburg effect, which is the suppression of oxidative metabolism in the presence of sufficient oxygen content. It was originally believed that the reduction in oxidative metabolism was due to the damaged mitochondria, but

this has since been refuted (Diaz-Ruiz et al. 2008). If LLC-PK_1 cells are displaying the Crabtree effect, then it would be possible to metabolically reprogram them by reducing the glucose concentration and/or improving the media content.

An article published by Weidemann and Krebs (1969), demonstrated that added acetoacetate and butyrate provided 80% of respiratory fuel for kidney cortex slices of male rats. Added glucose (5 mM) only provided 25-30% of the respiratory fuel (Weidmann and Kreb 1969). Some parts of the nephron such as the thick ascending limb of the loop of Henle, use glucose as its metabolic substrate. However, there is a reduced rate of respiration in proximal tubules when glucose is the only exogenous substrate (Mandel 1986).

What is of more importance is their ability to compensate for mitochondrial dysfunction by utilizing glycolysis for ATP generation. Hence, these cultured cells are more resistant to mitochondrial toxicities. Immortalized cell lines that are widely used for *in vitro* toxicity testing have evolved to grow and survive in hypoxic environments and fulfill their energy requirements via glycolysis instead of oxidative phosphorylation. Thus, many mitochondrial toxicants fail to impact mitochondrial function and cell viability in such cell lines because of this adaptation (Wills et al. 2015).

Complemented Media and Oxidative metabolism

Mitochondrial toxicity often serves as the primary mechanism of toxicity for most consumer products such as pesticides and pharmaceuticals (Wills 2017). Proximal tubular cells are enriched with a high mitochondrial density due to the

active transport of sodium. This feature makes the kidney especially sensitive to mitochondrial toxicants. Therefore, it is important to utilize an *in vitro* model that relies on oxidative phosphorylation to increase predictability.

One method of achieving this outcome is to modify the energy substrate content of the growth media. *In vitro* culture models, including LLC PK_1, are cultured in media that contain glucose as the main carbon source of energy. Addition of glucose to culture media of ascite AS-30D hepatoma cells lowered the pH, stimulated an increase in glycolytic enzymes and led to an inhibition of oxidative phosphorylation (Rodriguez-Enriquez et al. 2001). This suggests that current culture conditions where glucose is the main substrate will stimulate an increase in glycolytic activity with a concomitant decrease in mitochondrial respiration. HEPG2 cells cultured in DMEM with 25 mM glucose tolerated up to 1 μM of Rotenone without significant loss in viability (Marroquin et al. 2007). LLC-PK_1 cells showed an increase in glycolytic enzymes when glucose concentrations increased to 25 mM (Gstraunthaler et al. 1999).

Media modulation has been shown to improve oxidative metabolism of primary proximal tubular cells. In a study by Nowak and Schnellmann (1996), primary rabbit proximal tubular cells were cultured in medium that consisted of 50:50 mixture of DMEM and Ham's F-12, 5.5 mM glucose and 50 μM ascorbate-2-phosphate. The combination of low glucose (5.5 mM) and ascorbate stimulated an increase in basal oxygen consumption by 39% when compared to cells cultured in 5 mM only.

Media modulation has also been effective in metabolically reprogramming immortalized liver and skeletal muscle cells. Oleic acid (albumin conjugate) in the presence of 5 mM glucose, increased oxidative metabolism by stimulating an increase in the genes associated with fatty acid oxidation (Lim et al. 2013). Hepa 1.6 liver cells, grown in DMEM complemented with 5.5 mM glucose and 30 μM oleic acid were able to increase mitochondrial bioenergetic activity (Andreux et al. 2014). Fatty acid complemented media can represent a viable option as fatty acid beta- oxidation, takes place in the mitochondria and will utilize oxidative pathways to generate ATP. Previous work in our lab made attempts to culture LLC PK_1 cells in growth media complemented with oleic acid. However, oleic acid did not significantly alter the mitochondrial or glycolytic function. Thus, fatty acid complemented media were ineffective at reducing glycolysis and stimulating oxidative metabolism in LLC-PK_1 cells.

Complementing culture media with other energy sources can increase oxidative metabolism. Galactose has been used to improve the mitochondrial respiration of liver cells. Hep G2 liver cells cultured in DMEM complemented with 10 mM galactose and no glucose stimulated an increase in basal respiration rates compared to cells in 25 mM glucose (Marroquin et al. 2008). Previous work in our lab utilized galactose complemented media. When LLC-PK_1 cells were cultured in the presence of 10 mM and 5 mM galactose +/- glucose, the morphology changed and cell proliferation was reduced.

Ketone bodies can be used as a source of energy and has been shown to metabolically reprogram pancreatic cell lines and tumors (Shukla et al.2014). Sodium 3-hydroxybutyrate reduced glucose uptake as well as a decreased expression of glycolytic enzymes (Shukla et al. 2014). Treatment of the S2-013 human pancreatic cell line with 20 mM sodium-3-hydroxybutyrate shifted the bioenergetics of this line by reducing the glycolytic flux. (Shukla et al.2014). Treatment with this ketone body also reduced glucose uptake by reducing the expression of the glucose transporter 1 (GLUT 1) (Shukla et al. 2014). Additionally, beta-hydroxybutyrate also reduced lactate secretion by reducing expression of the lactate dehydrogenase A (LDHA), a subunit of the lactate dehydrogenase enzyme. (Shukla et al. 2014). Previous studies in our lab evaluated the impact of 5 mM betahydroxybutyrate (BHB) complemented media on the mitochondrial function of LLC-PK_1 cells. BHB did not significantly increase mitochondrial function when compared to LLC-PK_1 cells grown in 5 mM glucose or 5 mM acetoacetate.

Additional compounds were assessed for potential impact on mitochondrial function. Previous studies done in our lab evaluated quercetin for its protective effect on epithelial to mesenchymal transition (EMT). Quercetin is a phenolic flavonoid, found in many fruits, that has antioxidant properties (Rayamajhi et al. 2013). Quercetin has been shown to improve mitochondrial function and stimulate mitochondrial biogenesis. Primary mouse hepatocytes treated with varying doses of quercetin for 24 hours showed an increase in mitochondrial function and oxidative metabolism (Kim et al. 2015). HEP G2 cells treated with 15 μM for 24 hours, demonstrated a significant increase in cytochrome C oxidase (COX IV) protein

expression (Rayamajhi et al. 2013). Quercetin induced mitochondrial biogenesis is accompanied by an increase in COX IV (Rayamajhi et al. 2013). Peroxisome proliferator-activated receptor-γ coactivator (PGC)-1α (PGC-1α) is a master regulator of the transcriptional network that regulates mitochondrial biogenesis (Rayamajhi et al. 2013). PGC-1α activates mitochondrial transcription factor A (TFAM) that is responsible for transcribing proteins involved in mitochondrial DNA (mtDNA) transcription (Rayamajhi et al. 2013). Mitochondrial DNA encodes for subunits of the electron transport chain (Rayamajhi et al. 2013). Therefore, an increase in PGC-1α expression stimulates an increase in TFAM expression which results in an increase in ETC subunits such as COX IV.

Thus, there was a rationale to complementing the culture media with acetoacetate and quercetin to alter the bioenergetic activity of LLC PK_1 cells. Metabolic reprogramming of this cell line will be examined via the assessment of mitochondrial and glycolytic function, mitochondrial content and sensitivity to mitochondrial toxicants. Given these findings we proposed that complementing culture media with ketone bodies will alter the bioenergetic activity of the LLC-PK_1 line resulting in an increase in oxidative metabolism

Purpose of the study

This study will determine if media complementation will alter energy metabolism of LLC-PK_1 cells and increase the sensitivity to toxicants. Complementing the media with additional substrates may diminish the Crabtree effect, reducing glycolytic activity while increasing mitochondrial function. Two

preliminary studies were conducted, the results of which led to three formal hypotheses. To effectively study the impact of low glucose concentration on mitochondrial and glycolytic parameters, glucose concentration was lowered from 17.5 mM to 5 mM and the mitochondrial and glycolytic function was assessed via extracellular flux analysis (Seahorse Agilent ^{TM}). To evaluate the effect of media modulation on the metabolism of LLC-PK_1 cells, culture media were complemented with 5mM or 2 mM glucose in the presence or absence of acetoacetate or quercetin. Mitochondrial function was assessed via extracellular flux analysis. The results of the glucose and media modulation resulted in the three hypotheses with six specific aims.

Hypotheses

First hypothesis

Acetoacetate complemented culture media stimulates metabolic reprogramming of LLC-PK_1 cells by increasing mitochondrial function with a compensatory decrease in glycolytic function.

To adequately test this hypothesis, there were two specific aims:

1. To determine via extracellular flux analysis whether supplementation with 5 mM acetoacetate in the presence of 5 mM glucose affects the mitochondrial activity of LLC-PK_1 cells.
2. To examine via extracellular flux analysis whether complementation with 5 mM acetoacetate in the presence of 5 mM glucose affects the glycolytic activity of LLC-PK_1 cells.

Second hypothesis

Acetoacetate in the presence of 5 mM glucose stimulates an increase in mitochondrial content.

To adequately test this hypothesis, there was one specific aim:

1. To Determine whether acetoacetate stimulates an increase in markers of mitochondrial biogenesis and content.

Third hypothesis

5 mM acetoacetate in the presence of 5 mM glucose will sensitize LLC-PK1 cells to mitochondrial toxicants.

To adequately test this hypothesis, there were two specific aims:

1. To examine if acetoacetate supplementation alters the LC_{50} value of mitochondrial toxicants.
2. To evaluate if mitochondrial function of LLC-PK_1 cells cultured in acetoacetate complemented media are affected by mitochondrial toxicants.

Mitochondrial and Glycolytic assessment

Extracellular flux analysis detects small changes in the cell bioenergetics in real time by measuring changes in the oxygen consumption rate (OCR) and the extracellular acidification rate (ECAR). OCR measurements represent mitochondrial function by assessing the activity of the electron transport chain (ETC). ECAR measurements give a representation of glycolytic function. Mitochondrial function will be assessed by measuring the mitochondrial parameters *basal respiration*,

maximal respiration, *ATP-linked respiration* and *spare respiratory capacity* (figure 1). This tool will be used to extensively in this study to evaluate the effect of complemented media on bioenergetics. *Basal respiration* is the energetic demand of cell under baseline conditions, controlled by ATP turnover, substrate oxidation and proton leak (Brand and Nicholls 2011).

Maximal respiration is the maximal respiration rate in the presence of an uncoupler eg carbonyl cyanide-4-(trifluoromethoxy) phenylhydrazone (FCCP), which stimulates respiratory chain to operate at maximum capacity (Brand and Nicholls 2011). *ATP-linked respiration* is the rate of mitochondrial ATP synthesis under basal state/conditions. It represents the portion of basal respiration used to drive ATP synthesis (Brand and Nicholls 2011). Spare respiratory capacity is the ability of substrate supply and electron transport to respond to an increase in energy demand. It is the capability of the cell to respond to an energetic demand (Brand and Nicholls 2011).

Glycolytic function will be assessed by measuring the glycolytic parameters *glycolysis*, *glycolytic capacity* and *glycolytic reserve* (figure 2). In the flux analysis assay, *Glycolysis* is defined as the acidification rate that results from the addition of 25 mM glucose. This is the measure of the conversion rate of glucose to pyruvate or lactate (Mookerjee et al. 2016). *Glycolytic capacity* is the measurement is the maximum extracellular acidification rate reached by a cell following the addition of oligomycin, an ATP synthase inhibitor. This shuts down oxidative phosphorylation and driving the cell to use glycolysis to its maximum capacity (Mookerjee at al. 2016). *Glycolytic reserve* indicates the capability of a cell to respond to an energetic

demand as well as how close the glycolytic function is to the cell's theoretical maximum (Mookerjee et al. 2016).

Mitochondrial Assessment

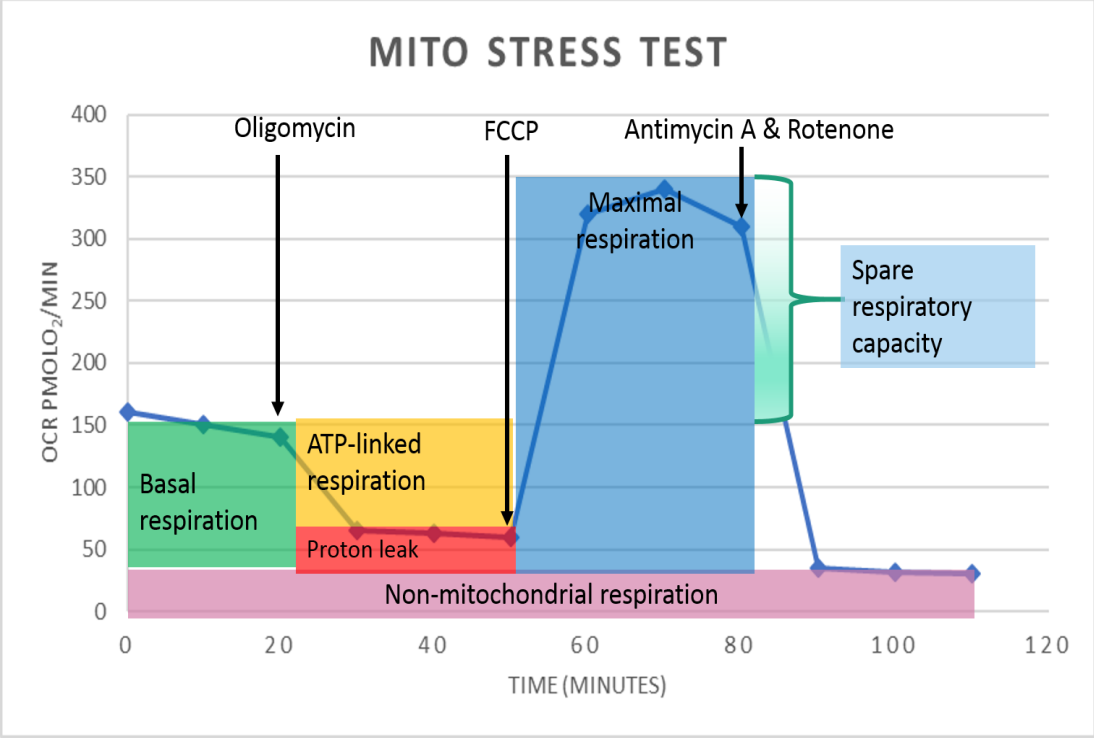

Figure 1: Mito Stress Test experimental design modified from Agilent

Mitochondrial Assessment

Parameter	**Description**
Basal Respiration	Energetic demand of cell under baseline conditions, controlled by ATP turnover, substrate oxidation and proton leak
Maximal Respiration	Maximum respiration rate in the presence of an uncoupler. Stimulates respiratory chain to operate at maximum capacity
ATP linked respiration	Rate of mitochondrial ATP synthesis under basal state/conditions. The portion of basal respiration used to drive ATP synthesis
Spare Respiratory Capacity	The ability of the substrate supply and electron transport chain to respond to an increase in energy demand. The ability of the cell to respond to an increase in energetic demand

Table 1: Measured mitochondrial parameters

Compound	**Effect**
Oligomycin	ATP Synthase/Complex V inhibitor. Useful to determine fraction of OCR used for ATP production
FCCP (carbonilcyanide p-triflouromethoxyphenylhydrazone)	Uncoupler. Used to calculate maximal respiration and spare capacity
Rotenone	Complex I inhibitor. Shuts down the electron transport chain (ETC) to calculate non-mitochondrial respiration

Antimycin A	Complex III inhibitor. Necessary for shutting down the ETC to calculate non-mitochondrial respiration

Table 2: Mito Stress Test protocol

Glycolytic Assessment

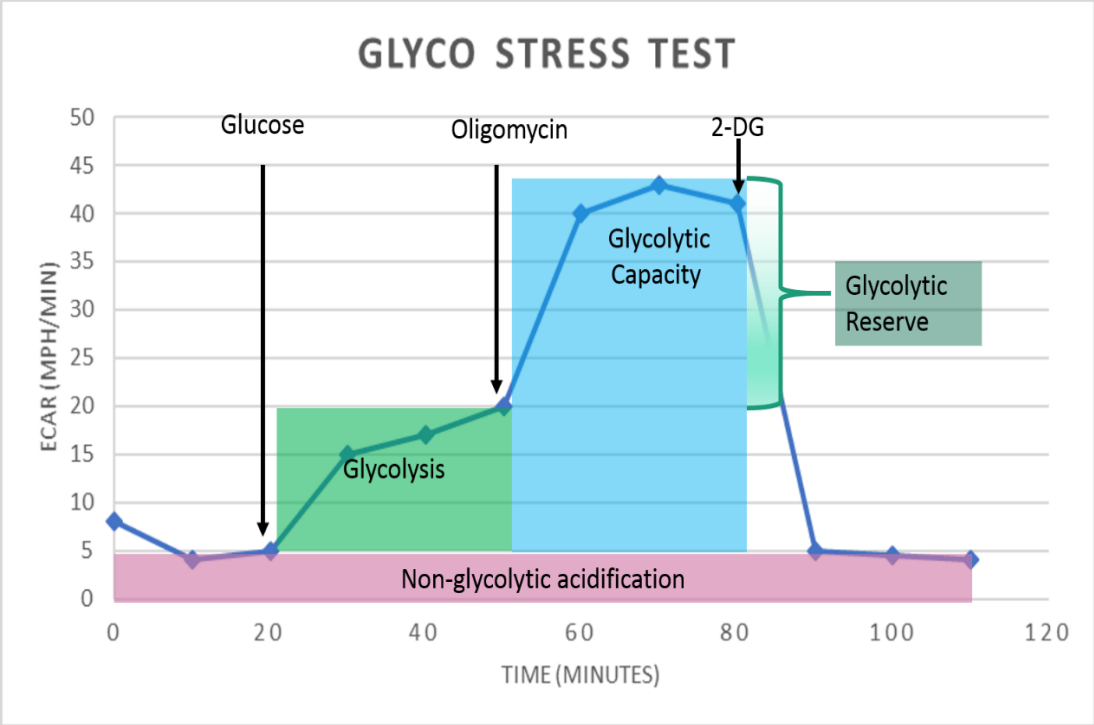

Figure2: Glyco Stress Test experimental design modified from Agilent

Glycolytic Assessment

Parameter	**Description**
Glycolysis	Acidification rate that results from the addition of 25 mM glucose. Measure of the conversion rate of glucose to pyruvate or lactate
Glycolytic Capacity	This measurement is the maximum ECAR reached by a cell following the addition of oligomycin, effectively shutting down oxidative phosphorylation and driving the cell to use glycolysis to its maximum capacity
Glycolytic Reserve	This measure indicates the capability of a cell to respond to an energetic demand as well as how close the glycolytic function is to the cell's theoretical maximum

Table 3: Measured glycolytic parameters

Compound	Effect
Glucose	Added after glucose starvation. Stimulates glycolysis
Oligomycin	ATP synthase/Complex V inhibitor. Stimulates an increased dependence on glycolysis to calculate glycolytic capacity

2-Deoxyglucose (2-DG)	Inhibits glycolysis. Necessary to calculate non-mitochondrial acidification

Table 4: Glyco Stress Test protocol

2. MATERIALS AND METHODS

Materials

Antimycin A (10189-312), FCCP (89156-962), oligomycin (80058-538), clotrimazole (AAJ63895-06), 96 well solid back flat bottom plates (29444-018) and Cayman MitoCheck® Citrate Synthase Activity assay (75817-190) were purchased from VWR. Trypan blue (0.4%) in PBS (Corning 25-900-CL), rotenone (361650), quercetin (50-498-664), lithium acetoacetate (A1478), and 2-deoxy glucose (11198-0010) were purchased from Fisher. Diclofenac sodium salt (D6899-10G, 0.5% triton X-100 (Sigma T8787) and D-glucose (G0721-1KG) were purchased from Sigma Aldrich. All antibodies for western blotting PGC-1α (3G6) (rabbit mAb #2178), COX IV (3E11) (rabbit mAb #4850) and GAPDH (14C10) (Rabbit mAb #2118) were purchased from Cell Signaling. Western blot analysis conducted using the Simple Protein Wes separation assay module SM-W004, and the anti-rabbit detection module DM-001 was purchased from Protein Simple.

Cell Culture

LLC-PK_1 clone 5 isolated by Dr. S. Ford in 1990 from the established cell line obtained from ATCC were grown on BD Falcon™ polystyrene tissue culture dishes (Thermo Fisher Scientific Cat# 353003) and maintained in the custom culture medium reconstituted to the standard SFFD composition with the exception of

glucose. The growth medium was a custom formula based on 50:50 DMEM: Ham's nutrient F12 with 15 mM HEPES, lacking phenol red (GIBCO custom formula, F# 91-5173 EL). It was reconstituted with ultra-pure water and the appropriate components to pH 7.4 and the addition of 2.5 mM L-glutamine and 0.5 mM sodium pyruvate with 3% fetal bovine serum (FBS) (Hyclone Thermo Scientific; cat # SH30070.03).

Antibiotics were not used. The medium was complemented with the following: glucose (2 mM, 5 mM, or 17.5 mM), quercetin (15 μM), acetoacetate (5 mM) or combinations of different substrates. The osmolality of the medium, +/- glucose, was 317 mOsm/kg. Cells used in experiments were between passages 240 and 260 and were maintained at 37ºC in an atmosphere of 95% air to 5% CO_2. The medium in the tissue culture plate was changed every three days after inoculation and the cells were subcultured on the fourth day after inoculation. Subculturing was done by trypsinizing the cells with trypsin-EDTA (Gibco by Life Technologies; ref # 15400-054) and split at a ratio of 1:5 or 1:10. The cultures were periodically checked for mycoplasma (Bionique Laboratories; Cat# M100). All experiments were carried out on confluent monolayers, determined by the presence of domes.

Extracellular flux analysis

LLC-PK_1 cells were seeded into an 8 well extracellular flux mini culture plate (Agilent 103025-100) at a density of 8×10^4 cells/well and grown in the respective growth medium for 48 hours to achieve confluency. Cells were seeded into 6 of the 8 wells, leaving the first and last well for background readings. The Mito Stress test or Glyco Stress test protocol was then used.

Mito stress test

Growth medium was then removed, and the cells were washed twice with 200 µL of Agilent XF base assay medium (102353-100) supplemented with either 17.5, 5, or 2 mM glucose, 2.5 mM glutamine and 0.5 mM sodium pyruvate. The medium was titrated with 0.2N of sodium hydroxide (NaOH) to adjust the pH to 7.4.

It was then filter sterilized and gently warmed until ready for use. A final volume of 180 µL was added to all 8 wells and the plate was then placed in a non-CO2 incubator. This was done at least 45 minutes before the start of the assay. XFp sensor cartridges (Agilent 103022-100) contain fluorophores that are quenched by oxygen and protons. These cartridges were soaked in the Seahorse XF calibrant solution (102353-100) the day before the assay and placed in a non-CO_2 incubator. On the day of the assay a pre-soaked cartridge was loaded according the Mito Stress test protocol (Brand and Nicholls 2011) as follows: port A- 20 µL of 1 µM Oligomycin; port B- 22 µL of 1 µM FCCP; port C- 25 µL of 0.5 µM Antimycin A and 0.5 µM Rotenone mix. The oxygen consumption rate (OCR) and extracellular acidification rates were then recorded using the Seahorse Xfp analyzer (Agilent Technologies). The analyzer was switched on and warmed up 6 hours before the start of the assay.

Glyco stress test

The cells were seeded according to the previously mentioned method listed under extracellular flux analysis. Growth medium was then removed and the cells were washed twice with 200 µL of Agilent XF base assay medium (102353-100) supplemented with 2.5mM glutamine. The medium was titrated and filtered according

to the Mito stress test protocol. The cells and cartridges were also prepared according to Mito Stress Test protocol. On the day of the assay, a pre-soaked sensor cartridge was loaded according the Glyco Stress test protocol (Mookerjee et al. 2016) as follows: port A- 20 µL of 25 mM glucose; port B- 22 µL of 1 µM oligomycin; port C- 25 µL of 50 mM 2-deoxyglucose. The extracellular acidification rates (ECAR) were then recorded using the Seahorse Xfp analyzer (Agilent Technologies).

Mito stress test-Respirometric Analysis (acute effect of toxicants on mitochondrial function)

LLC-PK_1 cells were seeded into an 8 well extracellular flux mini culture plate (Agilent 103025-100) at a density of 8×10^4 cells/well and grown in the respective growth medium for 48 hours to achieve confluency. A Mito stress test was conducted, and cells were exposed to the determined LC_{50} values from the 24hr viability study. Compounds that inhibited the electron transport chain (clotrimazole and ciprofibrate), were added in the final port (port C) of the cartridge (figure 3). Given that diclofenac acts as an uncoupler (Moreno-Sanchez et al.1999), it was added to second port (port B) where it will uncouple respiration following exposure to oligomycin. To confirm its activity as an uncoupler, 1 µM of FCCP was added to port C to observe any impacts on OCR (figure 4).

Extracellular flux data analysis and interpretation

Both OCR and ECAR readings were interpreted using the Wave software (version 2.2.0). Once the plate is removed the cells are washed with PBS and then lysed with 140uL of 0.2N NaOH. The cell lysates will be placed into 1.7mL eppendorf tubes and frozen at -20◦C until ready for use. The readings were then

normalized to DNA content assessed using the AccuBlue® Broad Range DNA Assay kit. 10 µL of cell lysates were added to 96 well solid black microplates (Corning 29444-018) followed by 200 µL of the AccuBlue® Broad Range working reagent. The working reagent contains 20 mL of the AccuBlue® Broad Range buffer followed by 200 µL of the AccuBlue® Broad range dye and 200 µL of the AccuBlue® Broad Range enhancer. Once sample and working reagent are added, the plate is placed in the dark for an incubation period of 10 minutes. Fluorescence is then measured using a microplate reader with 350 nm excitation/460 nm emission.

Assessment of Citrate Synthase activity

LLC-PK_1 were seeded at a density of 5×10^6 cells/mL into T225 tissue culture flasks (Corning 353139). Once confluent (20×10^6 cells), culture media were removed, and the cells were washed twice with ice-cold PBS, scraped, and pelleted by micro centrifugation at 350 × g at 4ºC for 5 minutes. To obtain whole cell lysates, cell pellets were lysed using Radio-Immune Precipitation assay (RIPA) buffer containing protease and phosphatase inhibitors for 30 min on ice and centrifuged at 140000 × g at 4ºC. 5 µL of lysates containing 5 µg of protein was used for the assay and diluted with 995 µL of the assay buffer.

The citrate synthase activity assay is a plate based colorimetric measurement in accordance with the Cayman MitoCheck® Citrate Synthase Activity Assay kit (701040). Citrate synthase activity is assessed via the formation of the tricarboxylate citrate that results from the condensation of oxaloacetate and acetyl CoA. The reaction is catalyzed by citrate synthase and yields SH-CoA. The product forms a yellow colored complex in the presence of Cayman MitoCheck® Citrate Synthase

Developing Reagent and measured at 412 nm. Absorbance is measured at 30 second intervals for 20 minutes. The results are graphed as the absorbance (y-axis) vs. time (minutes) (x-axis) and the slope of the linear portion of the curve is calculated. To determine the rate of reaction, the following equation is used:

$$\text{rate (mM/min)} = \frac{\text{slope (AU/sec)}}{\varepsilon\ \text{(AU/mM)}} \times 60\ \text{sec/min} \times \text{DF}$$

ε = 5.712 AU/mM

DF = 660

To determine the specific activity of the enzyme, the rate is divided by protein sample concentration (mg/mL).

Mitochondrial biomarker protein expression

LLC-PK_1 cells were seeded into T225 tissue culture flasks (Corning 353139). Once confluent (20×10^6 cells), culture media were removed and the cells were washed twice with ice-cold PBS, scraped, and pelleted by micro centrifugation. To obtain whole cell lysates, cell pellets were lysed using Radio-Immune Precipitation assay (RIPA) buffer containing protease and phosphatase inhibitors for 30 min on ice and centrifuged at 140000 × g at 4ºC. Protein expression was quantified by using WES, an automated capillary-based system with immunodetection (Protein Simple, Bio-Techne, US) by following manufacturer's instructions. Samples, at a concentration of 1 mg/ml were subjected to capillary electrophoresis followed by immunodetection. Proteins of interest were [PPAR (peroxisome proliferator-activated

receptor)-γ coactivator-1α] (PGC-1α), mitochondrial transcription factor A (TFAM), and cytochrome C oxidase (COX IV). Expression of protein of interest was normalized to expression of glyceraldehyde-3-phosphate dehydrogenase (GAPDH). The optimized antibody dilutions were as follows:

PGC-1α (1:100), TFAM (1:100), COX IV (1:100), and GAPDH (1:25000).

Cell viability assessment

Cell viability measured using a modified trypan blue-based viability assessment (Hammoudeh et al. 2019). Cells were seeded in 96 well plates at a density of 15×10^3 cells/well and allowed to grow until confluent monolayers were formed.

Cells were then treated for 24 hours with increasing concentrations of diclofenac (0.5 - 5mM), clotrimazole (0.1 – 100 µM) and ciprofibrate (1 - 40 µM). The treatment media were removed and the culture plate washed with PBS to remove dead cells, leaving only viable cells attached to the plate. The cells were first fixed with 4 % paraformaldehyde (Electron Microscopy Sciences 157-10) for twenty minutes, then permeabilized using 0.5% Triton X-100 (Sigma T8787) for 15 minutes. The cells were stained with 0.4% trypan blue in PBS (Corning 25-900-CL) for 30 minutes. Once staining was complete, the dye was removed, and cells were washed twice with PBS to remove any remaining trypan blue. The absorbance of the remaining viable cells was read at 530 nm. Percent cell viability compared to controls was reported. The percent viability was plotted as % V.C. on the Y-axis and the concentration of the corresponding compound was plotted on the X-axis. Using this graph, the LC-50 was determined for each of the three afore-mentioned compounds.

Statistical analysis

Statistical analyses were conducted using the GraphPad Prism version 5 (GraphPad Software, La Jolla CA, USA). For media complementation with varied nutrients and substrates, a one-way analysis of variance (ANOVA) was carried out using a Dunnett's multiple comparison post-hoc analysis where all groups were compared to the selected control 5 mM glucose group. For cells cultured in 17.5 mM or 5 mM glucose as well as cells cultured in 5 mM glucose or 5 mM glucose + 5 mM acetoacetate, a student's unpaired t-test was used to determine the significance of differences between two groups. Non-linear regression analysis was used to determine LC_{50} values. All data are represented as means ± SEM. Differences were statistically significant if p value was less than 0.05.

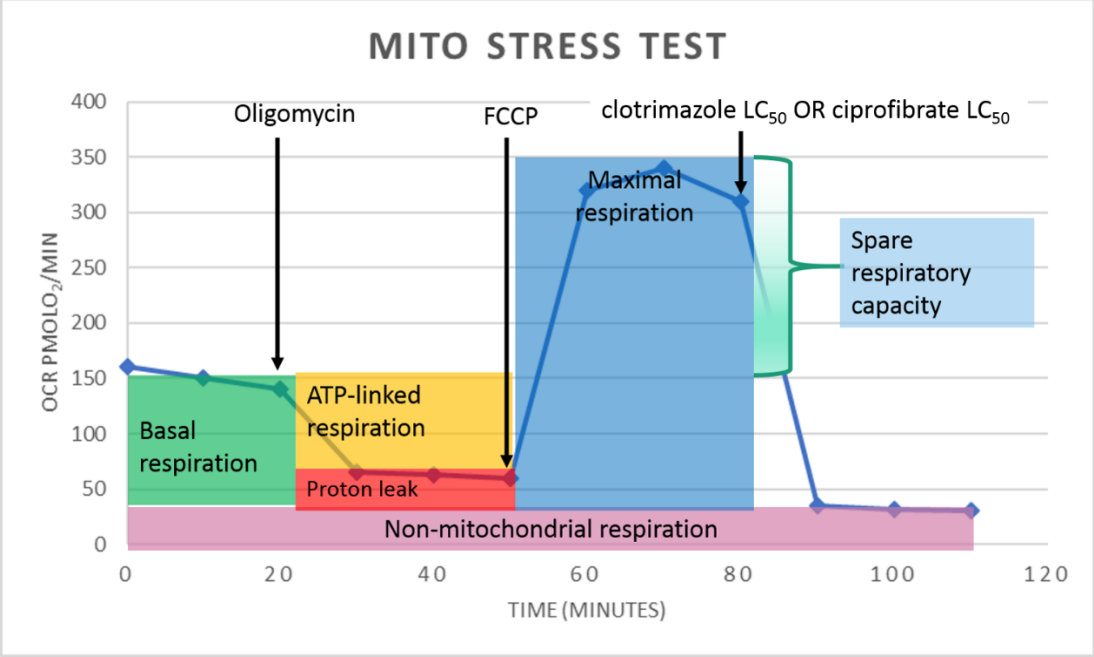

Figure 3: Mito Stress Test protocol for clotrimazole and ciprofibrate modified from Agilent

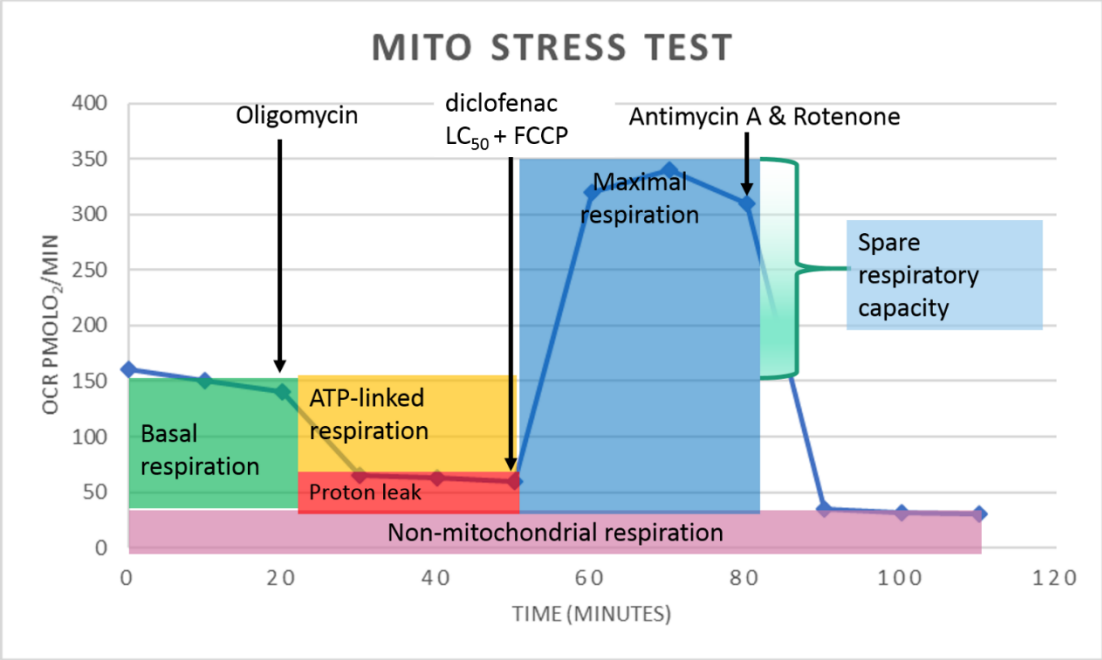

Figure 4: Mito Stress Protocol for diclofenac modified from Agilent

3. RESULTS

To examine the effect of lowering the glucose concentration on mitochondrial function, cells were cultured in 5 mM glucose or 17.5 mM glucose complemented medium. Mitochondrial function was assessed via the Seahorse Mito ™ Stress Test and the oxygen consumption rates (OCR) were recorded using the Seahorse Xfp analyzer. Lowering the glucose concentration from 17.5 mM to 5 mM, did not induce changes in any of the measured mitochondrial parameters. There was no change in basal respiration for cells grown in 5 mM and 17.5 mM glucose (figure 5). ATP-linked respiration (figure 6), maximal respiration (figure 3) and spare respiratory capacity (Figure 4) showed no significant differences between the two glucose groups.

Cells cultured in 5 mM glucose or 17.5 mM glucose medium were assessed for glycolytic function via the Agilent-Seahorse Glyco ™ Stress Test and the extracellular acidification rates (ECAR) were then recorded using the Seahorse Xfp analyzer (Agilent Technologies). Lowering the glucose concentration did not alter a change in the measured glycolytic parameters. There was no change in glycolysis (figure 7), glycolytic capacity (figure 8) or glycolytic reserve (figure 9).

Figure 5. Basal respiration for LLC-PK$_1$ cells grown in 5 mM and 17.5 mM glucose. LLC-PK$_1$ cells were seeded into an 8 well extracellular flux mini culture plate (Agilent 103025-100) at a density of 8×10^4 cells/well and grown in 5 mM or 17.5 mM growth medium for 48 hours to achieve confluency. The Agilent-Seahorse Mito Stress test protocol was then used and the oxygen consumption rates (OCR) were then recorded using the Seahorse Xfp analyzer and the results interpreted using the Wave 2.2.0 software. Basal respiration was calculated as the (last rate measurement before oligomycin) - (non-mitochondrial respiration). Statistical significance was determined using Student's unpaired t-test of five experiments.

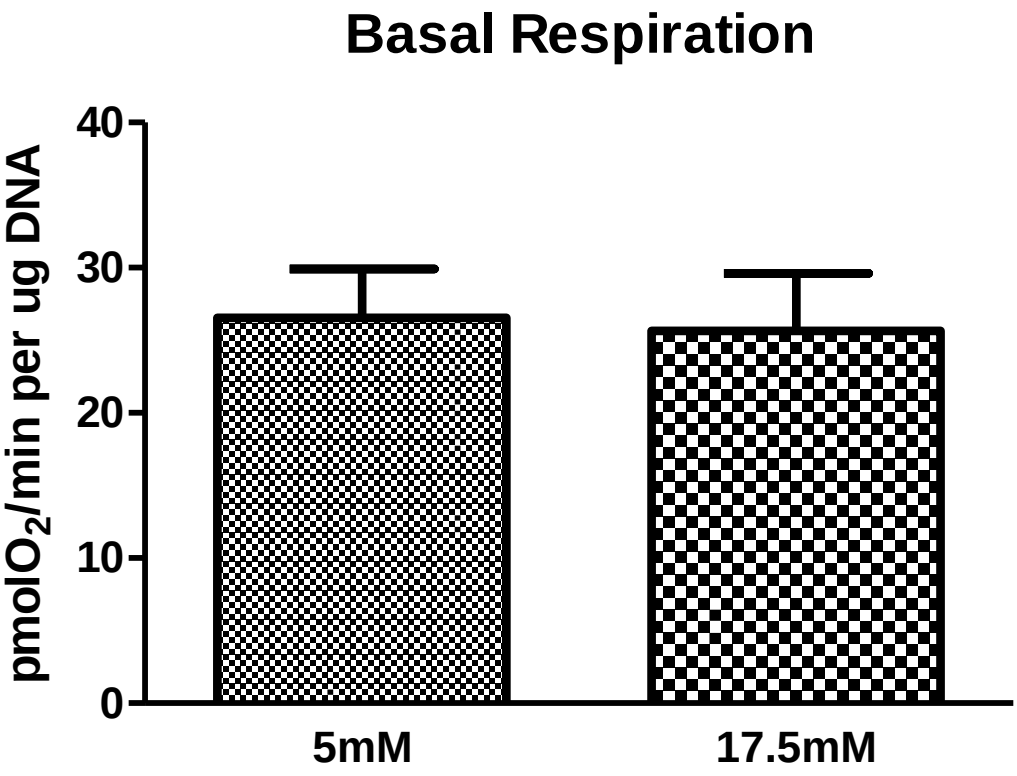
Basal Respiration
pmolO2/min per ug DNA
40
30
20
10
0
5mM
17.5mM

Figure 6. ATP-linked respiration for LLC-PK$_1$ cells grown in 5 mM and 17.5 mM glucose. LLC-PK$_1$ cells were seeded into an 8 well extracellular flux mini culture plate (Agilent 103025-100) at a density of 8×10^4 cells/well and grown in 5 mM or 17.5 mM growth medium for 48 hours to achieve confluency. The Agilent-Seahorse Mito Stress test protocol was selected and the oxygen consumption rates (OCR) were then recorded using the Seahorse Xfp analyzer and the results interpreted using the Wave 2.2.0 software. ATP-linked respiration was calculated as (last rate measurement before oligomycin injection)- (minimum rate measurement after oligomycin injection). Statistical significance was determined using Student's unpaired t-test of five experiments.

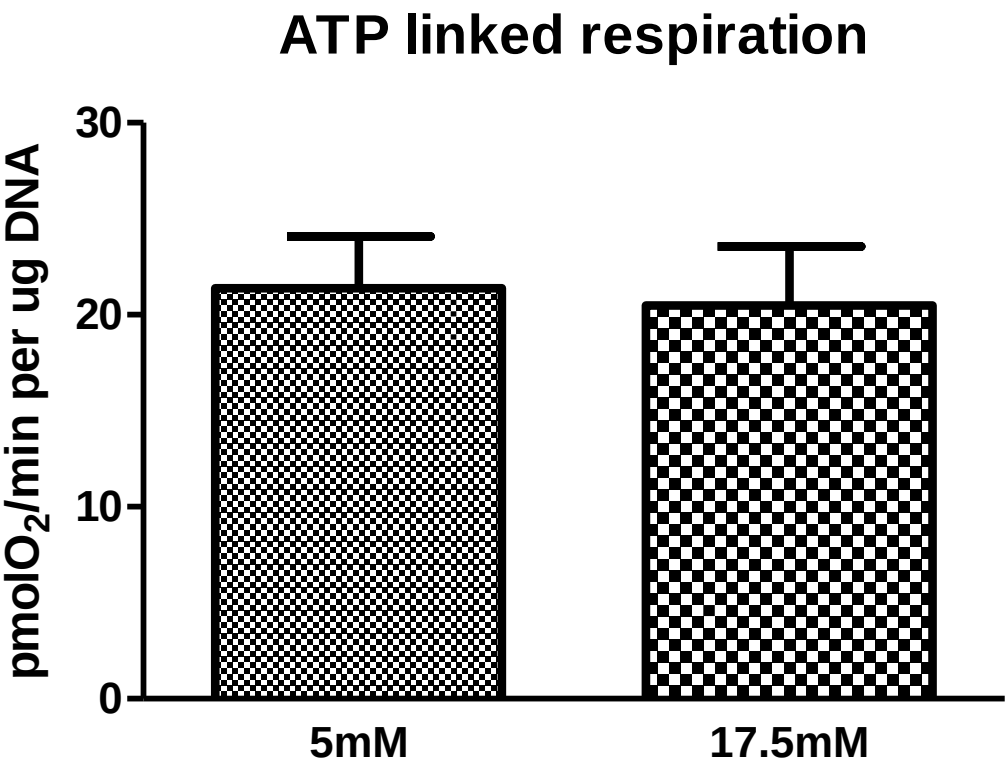
ATP linked respiration
pmolO2/min per ug DNA
30
20
10
0
5mM
17.5mM

Figure 7. Maximal respiration for LLC-PK$_1$ cells grown in 5 mM and 17.5 mM glucose. LLC-PK$_1$ cells were seeded into an 8 well extracellular flux mini culture plate (Agilent 103025-100) at a density of 8×10^4 cells/well and grown in 5 mM or 17.5 mM growth medium for 48 hours to achieve confluency. The Agilent-Seahorse Mito Stress test protocol was selected, and the oxygen consumption rates (OCR) were then recorded using the Seahorse Xfp analyzer and the results interpreted using the Wave 2.2.0 software. Maximal respiration was calculated as (maximum rate measurement after FCCP injection) - (non-mitochondrial respiration). Statistical significance was determined using Student's unpaired t-test of five experiments.

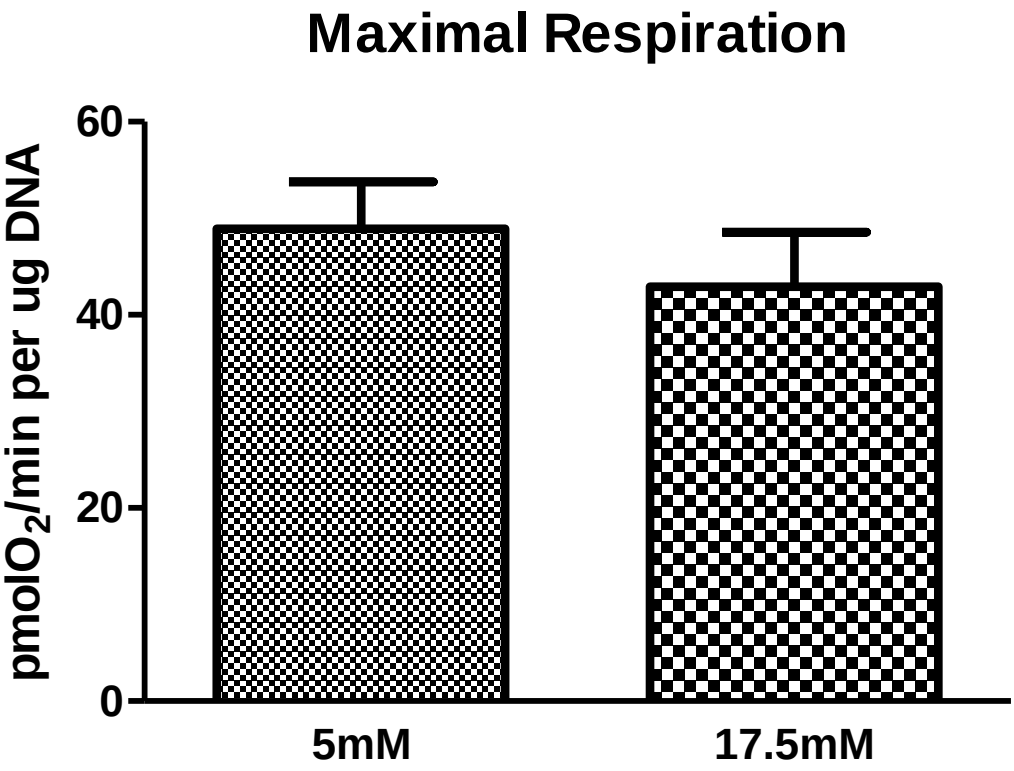
Maximal Respiration
pmolO2/min per ug DNA
60
40
20
0
5mM
17.5mM

Figure 8. Spare Respiratory Capacity for LLC-PK$_1$ cells grown in 5 mM and 17.5 mM glucose. LLC-PK$_1$ cells were seeded into an 8 well extracellular flux mini culture plate (Agilent 103025-100) at a density of 8×10^4 cells/well and grown in 5 mM or 17.5 mM growth medium for 48 hours to achieve confluency. The Agilent-Seahorse Mito Stress test protocol was selected, the oxygen consumption rates (OCR) were then recorded using the Seahorse Xfp analyzer and the results interpreted using the Wave 2.2.0 software. Spare respiratory capacity was calculated as (maximal respiration) - (basal respiration). Statistical significance was determined using Student's unpaired t-test of five experiments.

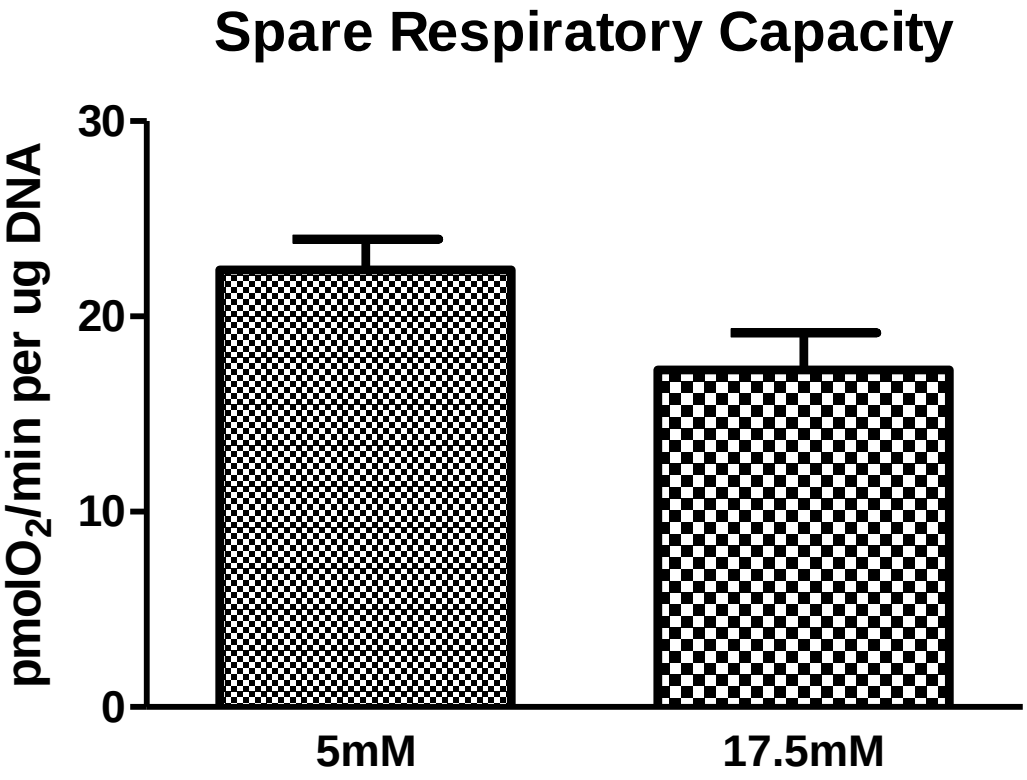
Spare Respiratory Capacity
pmolO2/min per ug DNA
30
20
10
0
5mM
17.5mM

Figure 9. Glycolysis for LLC-PK$_1$ cells grown in 5 mM and 17.5 mM glucose. Cells cultured in 5 mM glucose or 17.5 mM glucose medium were assessed for glycolytic function via the Agilent-Seahorse Glyco ^{TM} stress test once cells achieved 100% confluency, and the Glyco Stress test protocol was selected. The extracellular acidification rates (ECAR) were then recorded using the Seahorse Xfp analyzer (Agilent Technologies). Glycolysis was calculated as (maximum rate measurement before oligomycin injection) - (minimum rate measurement before glucose injection). Statistical significance was determined using Student's unpaired t-test of five experiments.

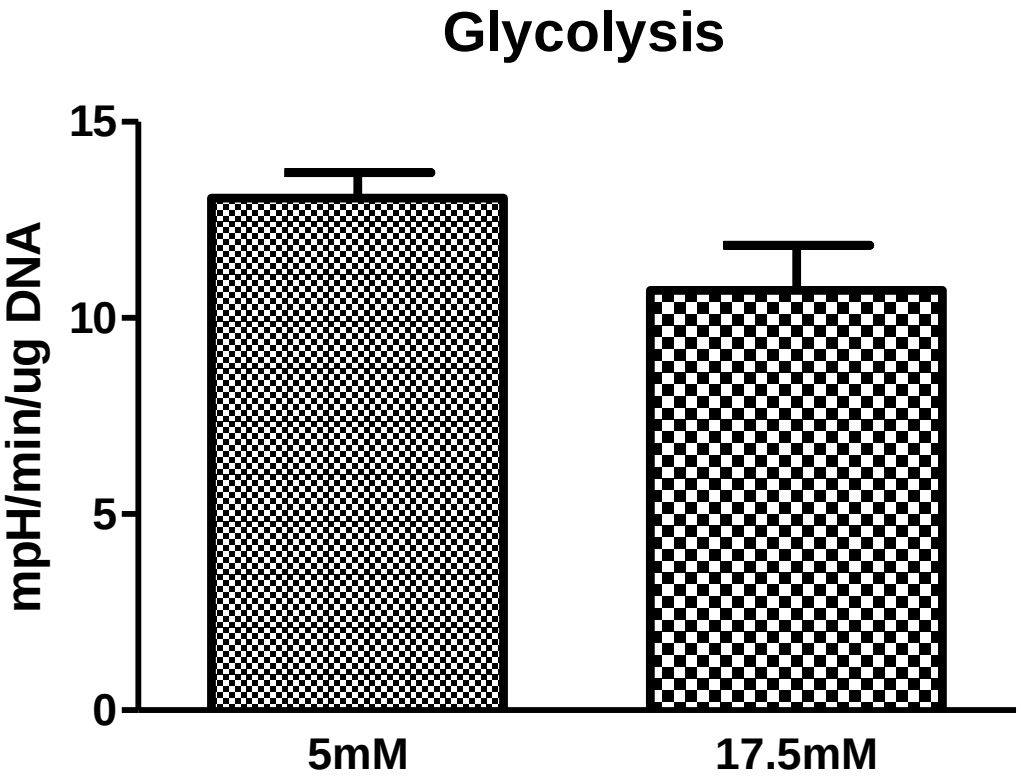
Glycolysis
mpH/min/ug DNA
15
10
5
0
5mM
17.5mM

Figure 10. Glycolytic Capacity for LLC-PK$_1$ cells grown in 5 mM and 17.5 mM glucose. Cells cultured in 5 mM glucose or 17.5 mM glucose medium were assessed for glycolytic function via the Agilent-Seahorse Glyco ^{TM} stress test once cells achieved 100% confluency. The Glyco Stress test protocol was used, and the extracellular acidification rates (ECAR) were then recorded using the Seahorse Xfp analyzer (Agilent Technologies). Glycolytic capacity was calculated as (maximum rate measurement after oligomycin injection) – (last rate measurement before glucose injection). Statistical significance was determined using Student's unpaired t-test of five experiments.

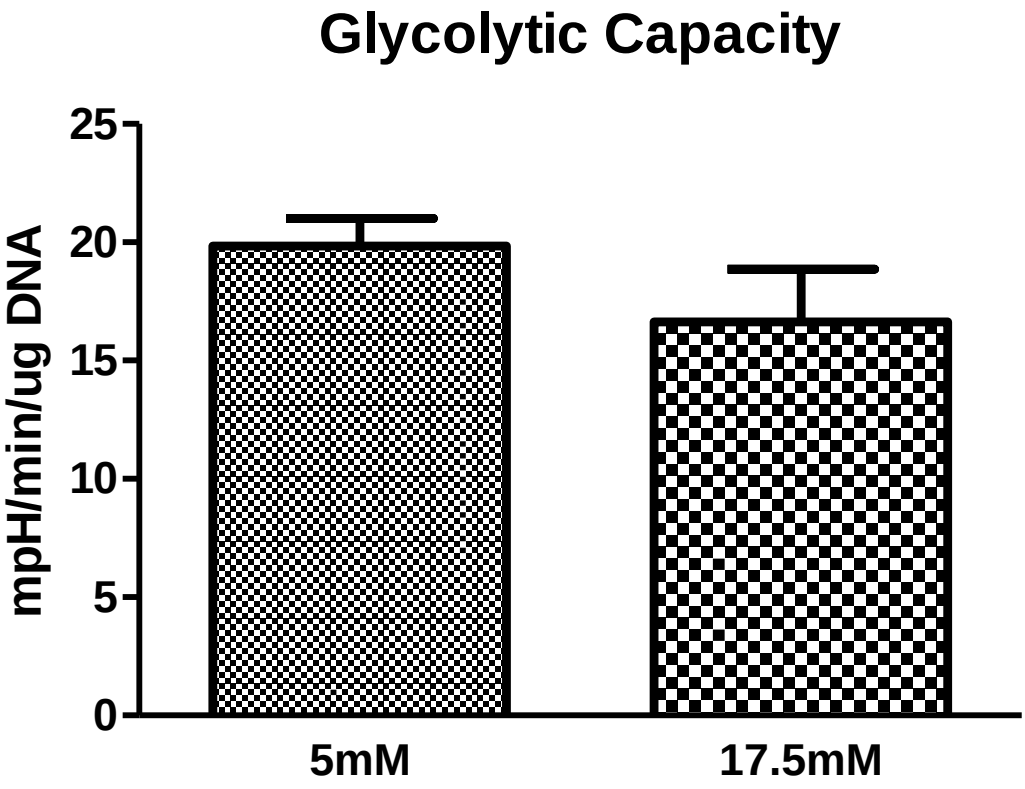
Glycolytic Capacity
mpH/min/ug DNA
25
20
15
10
5
0
5mM
17.5mM

Figure 11. Glycolytic Reserve for LLC-PK$_1$ cells grown in 5 mM and 17.5 mM glucose. Cells cultured in 5 mM glucose or 17.5 mM glucose medium were assessed for glycolytic function via the Agilent-Seahorse Glyco ™ stress test once cells achieved 100% confluency and the Glyco Stress test protocol was used. The extracellular acidification rates (ECAR) were then recorded using the Seahorse Xfp analyzer (Agilent Technologies). Glycolytic reserve was calculated as (glycolytic capacity) – (glycolysis). Statistical significance was determined using Student's unpaired t-test of five experiments.

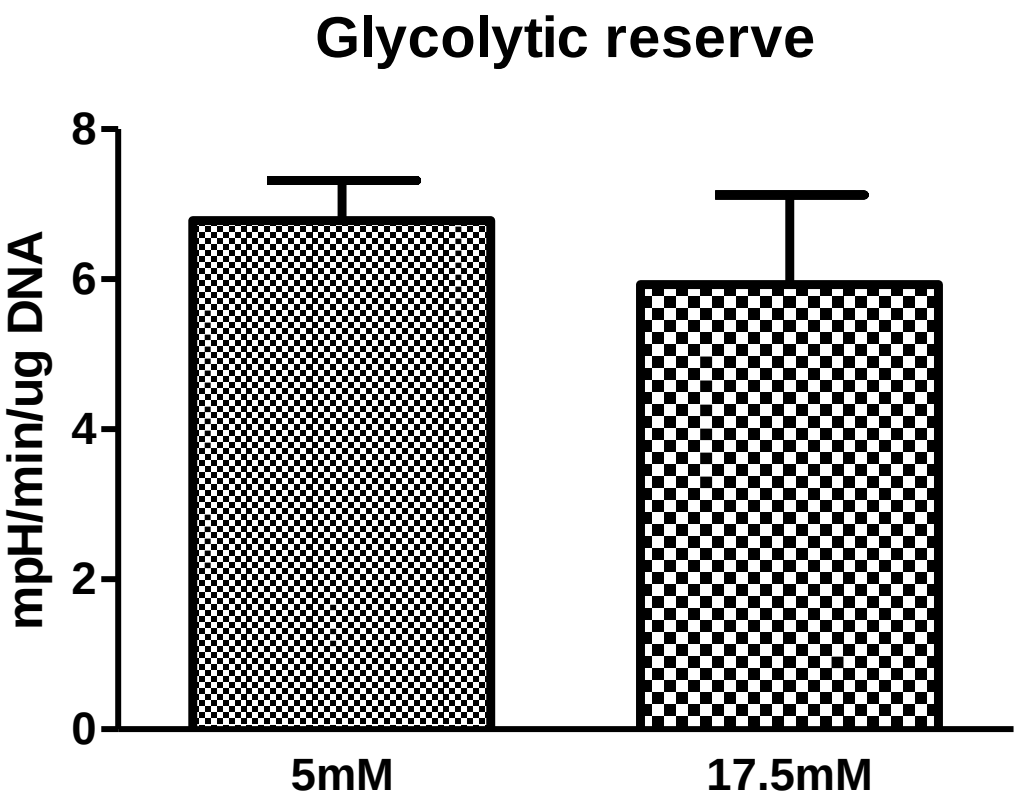
Glycolytic reserve
mpH/min/ug DNA
8
6
4
2
0
5mM
17.5mM

Reducing the glucose concentration from 17.5 mM to 5 mM did not significantly alter mitochondrial function. Thus, media modulation was utilized to stimulate an increase in mitochondrial function. Additional substrates were added to either 2 mM or 5 mM glucose complemented media. LLC PK_1 cells were cultured in either 5 mM (5G) or 2 mM (2G) glucose culture medium in the presence of 15 μM quercetin (5G15Q or 2G15Q), 5 mM acetoacetate (5G5A or 2G5A), both (2G5A15Q or 5G5A15Q) or without quercetin or acetoacetate. Mitochondrial assessment was determined via the Agilent-Seahorse Mito ^{TM} Stress Test and the oxygen consumption rates (OCR) were then recorded using the Seahorse Xfp analyze.

There were no differences in basal respiration (figure 12) or ATP-linked respiration (figure 13). However, there was a significant increase in maximal respiration (figure 14) and spare respiratory capacity (figure 15) in the 5G5A, and the 5G5A15Q group when compared to the control group, 5 mM glucose (5G). Maximal respiration for 5G5A (84.2 ± 9.0 pmol O2/ min/ug DNA) and the 5G5A15Q (88.5 ± 11.0 pmol O2/ min/ug DNA) was 45% and 53% higher respectively when compared to 5G (57.7 ± 7.8 pmol O2/min/ug DNA) only.

Figure 12. Basal respiration for LLC-PK$_1$ cells grown in media complemented with different glucose levels and different substrates. LLC-PK$_1$ cells were seeded into an 8 well extracellular flux mini culture plate at a density of 8×10^4 cells/well. The cells were cultured in either 5 mM (5G) or 2 mM (2G) glucose culture medium in the presence of 15 μM quercetin (5G15Q or 2G15Q), 5 mM acetoacetate (5G5A or 2G5A), both (5G5A15Q or 2G5A15Q) or without quercetin or acetoacetate for 48 hours to achieve confluency. The Agilent-Seahorse Mito Stress test protocol was then used, and the oxygen consumption rates (OCR) were then recorded using the Seahorse Xfp analyzer. Basal respiration was calculated as the (last rate measurement before oligomycin) - (non-mitochondrial respiration). Statistical significance was determined using one-way ANOVA, Dunnett's multiple comparison post hoc analysis of seven experiments.

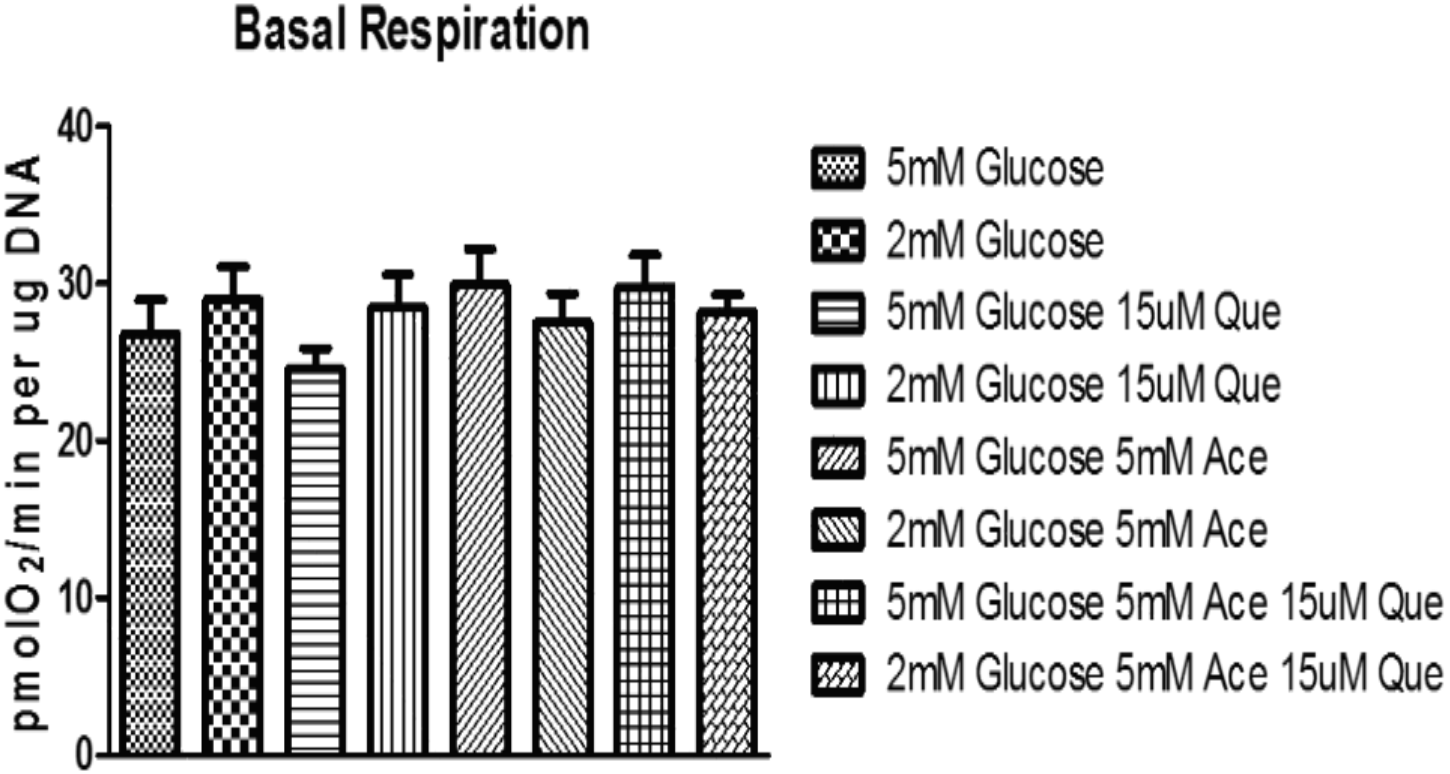
Basal Respiration
pmol O2/min per ug DNA
40
30
20
10
0
5mM Glucose
2mM Glucose
5mM Glucose 15uM Que
2mM Glucose 15uM Que
5mM Glucose 5mM Ace
2mM Glucose 5mM Ace
5mM Glucose 5mM Ace 15uM Que
2mM Glucose 5mM Ace 15uM Que

Figure 13. ATP-linked respiration for LLC-PK$_1$ cells grown in media complemented with different glucose levels and different substrates. LLC-PK$_1$ cells were seeded into an 8 well extracellular flux mini culture plate at a density of 8×10^4 cells/well. The cells were cultured in either 5 mM (5G) or 2 mM (2G) glucose culture medium in the presence of 15 μM quercetin (5G15Q or 2G15Q), 5 mM acetoacetate (5G5A or 2G5A), both (5G5A15Q or 2G5A15Q) or without quercetin or acetoacetate for 48 hours to achieve confluency and the Agilent-Seahorse Mito Stress test protocol was then used. The oxygen consumption rates (OCR) were then recorded using the Seahorse Xfp. ATP-linked respiration was calculated as (last rate measurement before oligomycin injection)- (minimum rate measurement after oligomycin injection). Statistical significance was determined using one-way ANOVA, Dunnett's multiple comparison post hoc analysis of seven experiments.

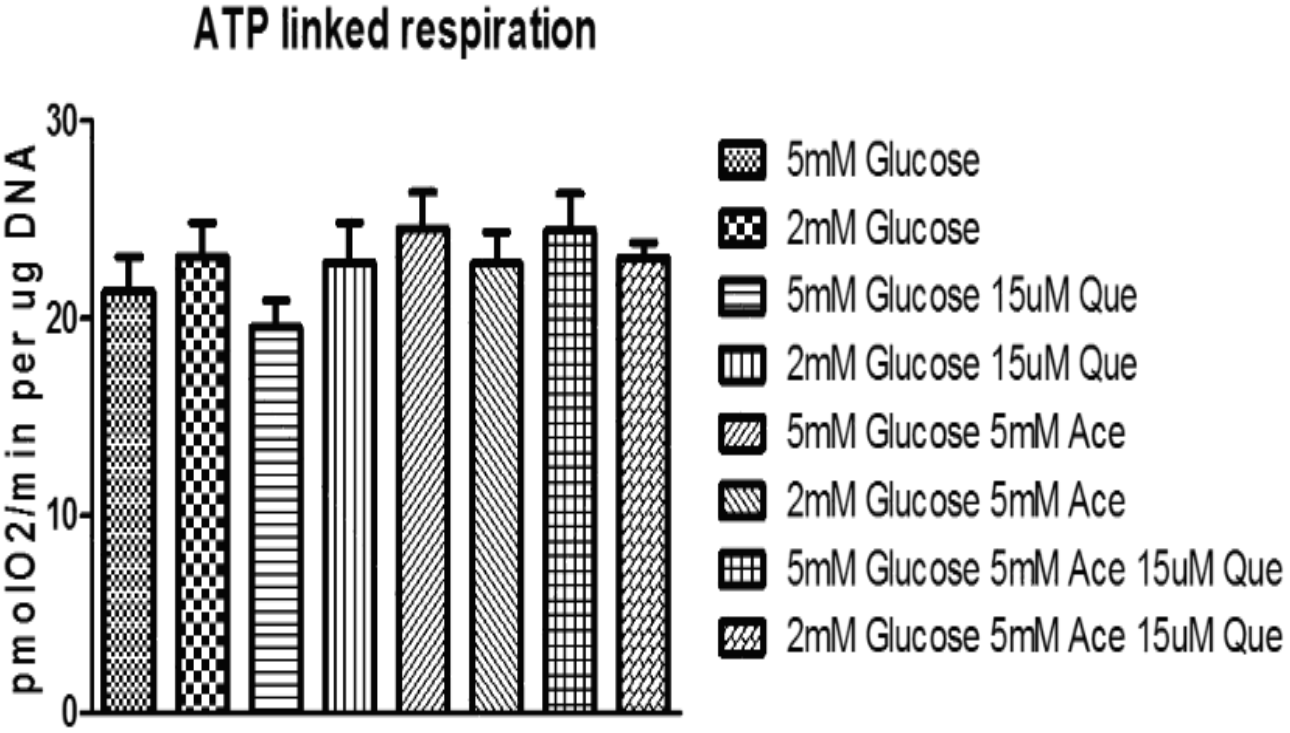
ATP linked respiration
pmolO2/min per ug DNA
30
20
10
0
5mM Glucose
2mM Glucose
5mM Glucose 15uM Que
2mM Glucose 15uM Que
5mM Glucose 5mM Ace
2mM Glucose 5mM Ace
5mM Glucose 5mM Ace 15uM Que
2mM Glucose 5mM Ace 15uM Que

Figure 14. Maximal respiration for LLC-PK$_1$ cells grown in media complemented with different glucose levels and different substrates. LLC-PK$_1$ cells were seeded into an 8 well extracellular flux mini culture plate at a density of 8×10^4 cells/well. The cells were cultured in either 5 mM (5G) or 2 mM (2G) glucose culture medium in the presence of 15 μM quercetin (5G15Q or 2G15Q), 5 mM acetoacetate (5G5A or 2G5A), both (5G5A15Q or 2G5A15Q) or without quercetin or acetoacetate for 48 hours to achieve confluency. The Agilent-Seahorse Mito Stress test protocol was then used, and the oxygen consumption rates (OCR) were then recorded using the Seahorse Xfp. Maximal respiration was calculated as (maximum rate measurement after FCCP injection) - (non-mitochondrial respiration). Statistical significance was determined using one-way ANOVA, Dunnett's multiple comparison post hoc analysis of seven experiments. $P<0.05$ (*), $P<0.01$(**)

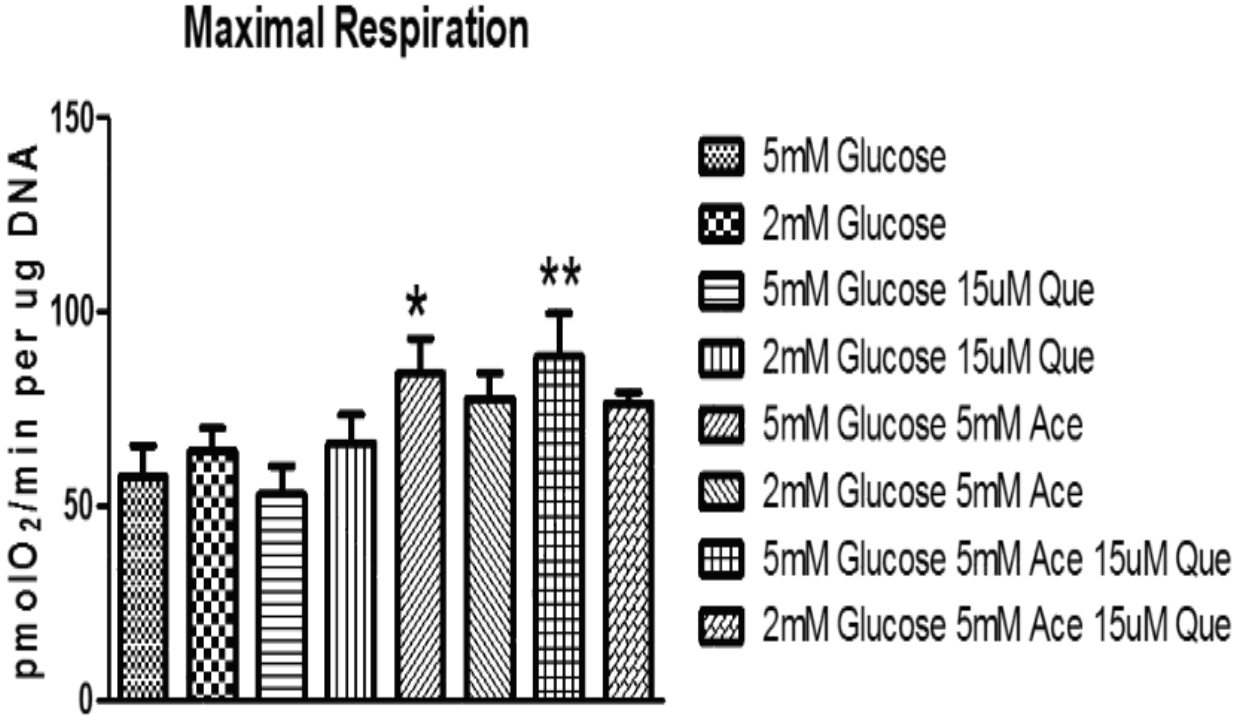
Maximal Respiration
pmolO2/min per ug DNA
150
100
50
0
*
**
5mM Glucose
2mM Glucose
5mM Glucose 15uM Que
2mM Glucose 15uM Que
5mM Glucose 5mM Ace
2mM Glucose 5mM Ace
5mM Glucose 5mM Ace 15uM Que
2mM Glucose 5mM Ace 15uM Que

Figure 15. Spare respiratory capacity for LLC-PK$_1$ cells grown in media complemented with different glucose levels and different substrates. LLC-PK$_1$ cells were seeded into an 8 well extracellular flux mini culture plate at a density of 8×10^4 cells/well. The cells were cultured in either 5 mM (5G) or 2 mM (2G) glucose culture medium in the presence of 15 μM quercetin (5G15Q or 2G15Q), 5 mM acetoacetate (5G5A or 2G5A), both (5G5A15Q or 2G5A15Q) or without quercetin or acetoacetate for 48 hours to achieve confluency. The Agilent-Seahorse Mito Stress test protocol was then used, and the oxygen consumption rates (OCR) were then recorded using the Seahorse Xfp analyzer. Spare respiratory capacity was calculated as (maximal respiration) - (basal respiration). Statistical significance was determined using one-way ANOVA, Dunnett's multiple comparison post hoc analysis of seven experiments. $P<0.05$(*), $P<0.01$(**)

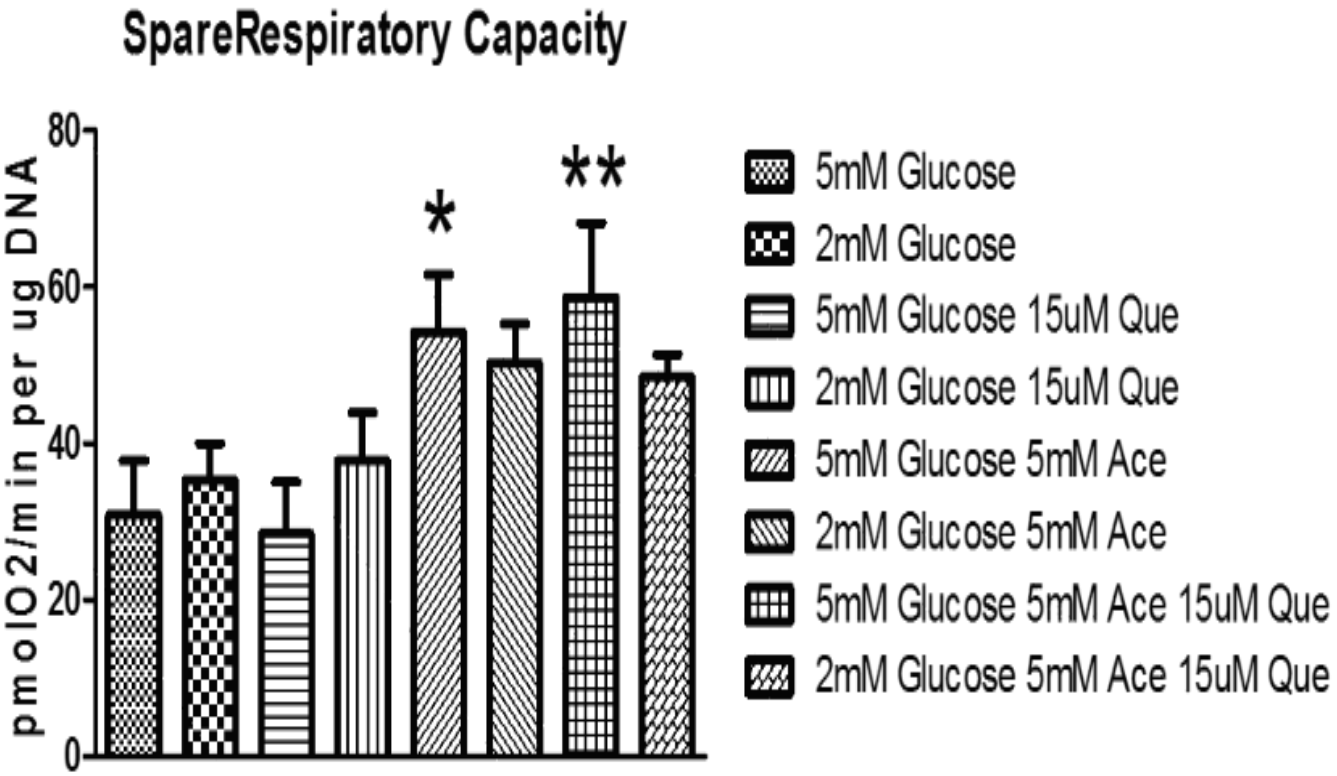
SpareRespiratory Capacity
pmolO2/min per ug DNA
80
60
40
20
0
*
**
5mM Glucose
2mM Glucose
5mM Glucose 15uM Que
2mM Glucose 15uM Que
5mM Glucose 5mM Ace
2mM Glucose 5mM Ace
5mM Glucose 5mM Ace 15uM Que
2mM Glucose 5mM Ace 15uM Que

Quercetin had no effect on mitochondrial function. Thus, we decided to examine whether the presence of 5 mM acetoacetate in culture medium will increase mitochondrial function. LLC-PK_1 cells were cultured in 5 mM glucose (5G) or 5 mM glucose and 5 mM acetoacetate (5G5A). Mitochondrial function was assessed via the Mito ^{TM} stress test. Cells in the acetoacetate complemented medium showed a 45% increase in basal respiration (29.5 ±4.1 pmol/min/ugDNA) when compared to 5G (20.2 ±1.9 pmol/min/ugDNA) (Figure 16). There was also a 63% increase in ATP linked respiration (24.7 ± 3.9 pmol/min/ugDNA) when compared to the 5G group (15.2 ± 1.7 pmol/min/ugDNA) (Figure 17). Maximal respiration increased by 110% (93.2 ± 11 pmol/min/ugDNA) in the 5G5A when compared to 5G (44.2 ± 4.2 pmol/min/ugDNA) (Figure 18). LLC PK_1 cells in 5G5A showed a 165% increase in spare respiratory capacity (63.7 ±7.9 pmol/min/ugDNA) when compared to cells in 5G group (24.1 ±2.3 pmol/min/ugDNA) (Figure 19). The results demonstrated that acetoacetate complemented medium produced a significant increase in the measured mitochondrial function.

Under conditions which increase mitochondrial function, the cells were also assessed for changes in glycolytic function. Cells were cultured in 5 mM glucose (5G) or 5 mM glucose + 5 mM acetoacetate (5G5A) complemented medium. Glycolytic function was determined via the Seahorse Glyco ^{TM} stress test once cells achieved 100% confluency. Although there is a trend, acetoacetate did not significantly lower glycolysis in the presence of high glucose concentration (figure 20). Acetoacetate in culture medium lowered the glycolytic capacity by 25% in the

5G5A medium (5G5A:17.2 ± 1.3 mpH/min/ugDNA, 5G: 22.8 ± 2. mpH/min/ugDNA) (figure 21).

There was also a 30% reduction in glycolytic reserve of cells in the 5G5A medium (5G5A: 5.44± 0.2 mpH/min/ugDNA, 5G:7.73 ± 0.58 mpH/min/ugDNA) (figure 22). These finding indicate that there is an increase in mitochondrial function.

Figure 16. Basal respiration for LLC-PK$_1$ cells grown in 5 mM acetoacetate. LLC-PK$_1$ cells were seeded into an 8 well extracellular flux mini culture plate at a density of 8×10^4 cells/well. The cells were cultured in either 5 mM glucose (5G) or 5 mM glucose + 5 mM acetoacetate (5G5A) for 48 hours to achieve confluency. The Agilent-Seahorse Mito Stress test protocol was then used, and the oxygen consumption rates (OCR) were then recorded using the Seahorse Xfp analyzer. Basal respiration was calculated as the (last rate measurement before oligomycin) - (non-mitochondrial respiration). Statistical significance was determined using Student's unpaired t-test of five experiments. $P<0.05$(*)

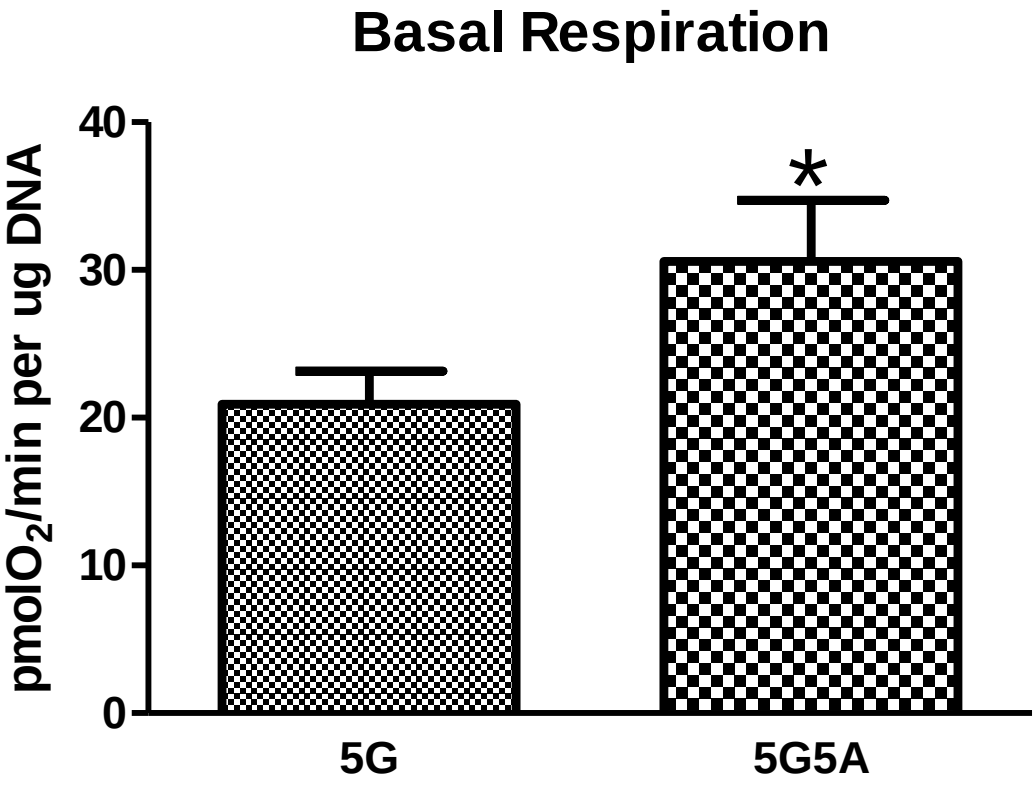
Basal Respiration
pmolO2/min per ug DNA
40
30
20
10
0
*
5G
5G5A

Figure 17. ATP-linked respiration for LLC-PK$_1$ cells grown in 5 mM acetoacetate. LLC-PK$_1$ cells were seeded into an 8 well extracellular flux mini culture plate at a density of 8×10^4 cells/well. The cells were cultured in either 5 mM glucose (5G) or 5 mM glucose + 5 mM acetoacetate (5G5A) for 48 hours to achieve confluency and the Agilent-Seahorse Mito Stress test protocol was then used. The oxygen consumption rates (OCR) were then recorded using the Seahorse Xfp analyzer. ATP-linked respiration was calculated as (last rate measurement before oligomycin injection)- (minimum rate measurement after oligomycin injection). Statistical significance was determined using Student's unpaired t-test of five experiments. $P<0.05$(*)

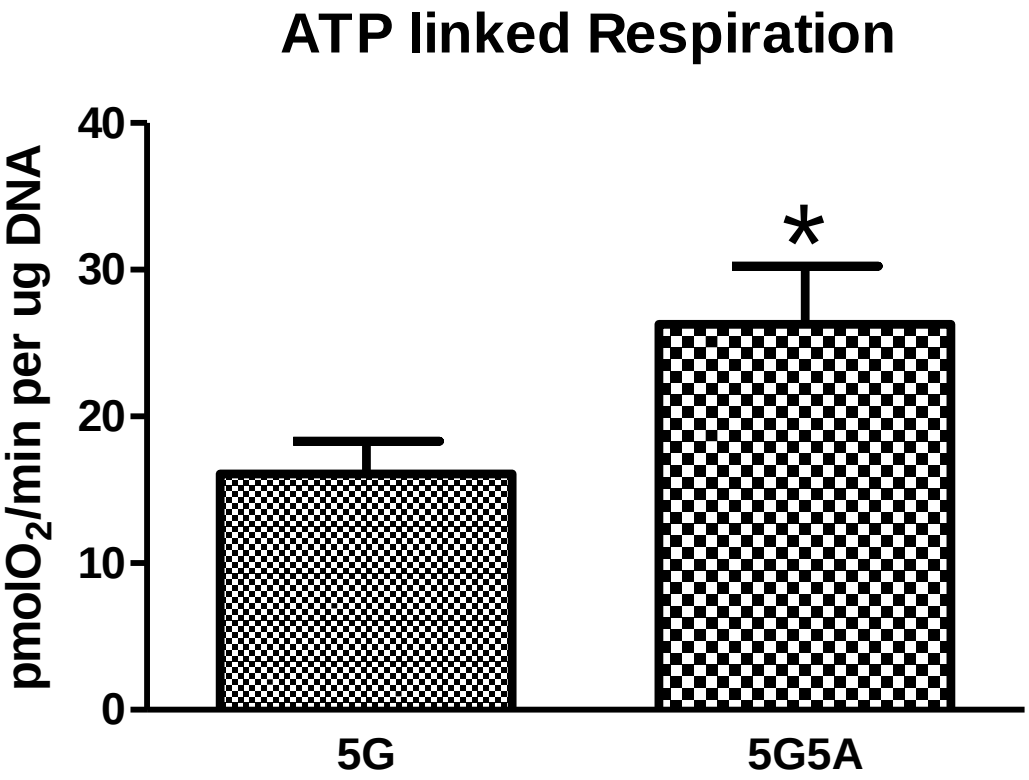
ATP linked Respiration
pmolO2/min per ug DNA
40
30
20
10
0
*
5G
5G5A

Figure 18. Maximal respiration for LLC-PK$_1$ cells grown in 5 mM acetoacetate. LLC-PK$_1$ cells were seeded into an 8 well extracellular flux mini culture plate at a density of 8×10^4 cells/well. The cells were cultured in either 5 mM glucose (5G) or 5 mM glucose + 5 mM acetoacetate (5G5A) for 48 hours to achieve confluency and the Agilent-Seahorse Mito Stress test protocol was then used. The oxygen consumption rates (OCR) were then recorded using the Seahorse Xfp analyzer. Maximal respiration was calculated as maximum rate measurement after FCCP injection) - (non-mitochondrial respiration). Statistical significance was determined using Student's unpaired t-test of five experiments. $P<0.01$(**)

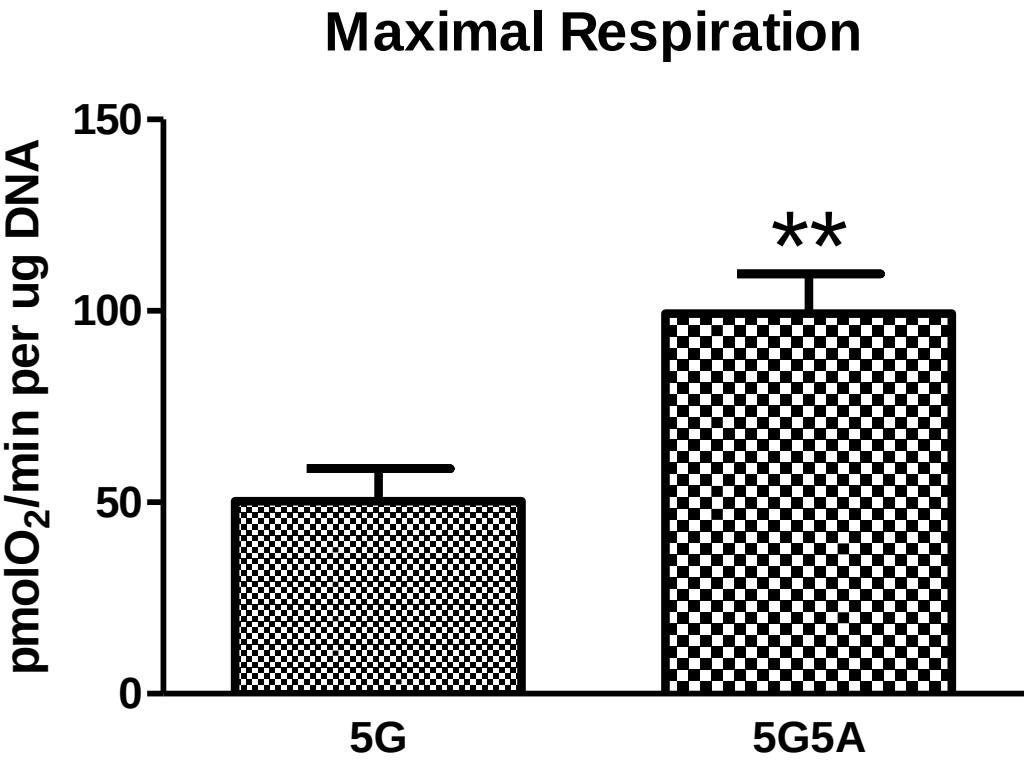
Maximal Respiration
150
100
50
0
pmolO2/min per ug DNA
**
5G
5G5A

Figure 19. Spare respiratory capacity for LLC-PK$_1$ cells grown in 5 mM acetoacetate. LLC-PK$_1$ cells were seeded into an 8 well extracellular flux mini culture plate at a density of 8×10^4 cells/well. The cells were cultured in either 5 mM glucose (5G) or 5 mM glucose + 5 mM acetoacetate (5G5A) for 48 hours to achieve confluency. The Agilent-Seahorse Mito Stress test protocol was then used, and the oxygen consumption rates (OCR) were then recorded using the Seahorse Xfp analyzer. Spare respiratory capacity was calculated as (maximal respiration) - (basal respiration). Statistical significance was determined using Student's unpaired t-test of five experiments. $P<0.01$(**)

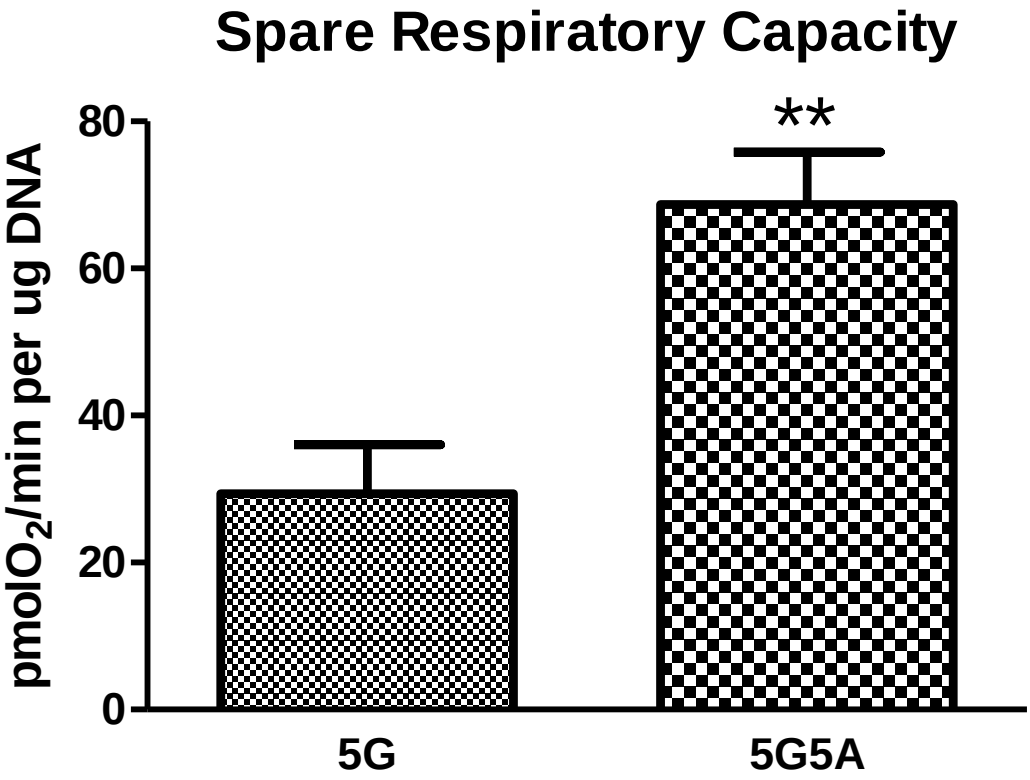
Spare Respiratory Capacity
pmolO2/min per ug DNA
80
60
40
20
0
**
5G
5G5A

Figure 20. Glycolysis for LLC-PK$_1$ cells grown in 5 mM acetoacetate. Cells cultured in 5 mM glucose (5G) or 5 mM glucose + 5 mM acetoacetate (5G5A) medium were assessed for glycolytic function via the Agilent-Seahorse Glyco ™ stress test once cells achieved 100% confluency and the Glyco Stress test protocol was used. The extracellular acidification rates (ECAR) were then recorded using the Seahorse Xfp analyzer (Agilent Technologies). Glycolysis is calculated as (maximum rate measurement before oligomycin injection) - (Minimum rate measurement before glucose injection). Statistical significance was determined using Student's unpaired t-test of five experiments. (P=0.0708)

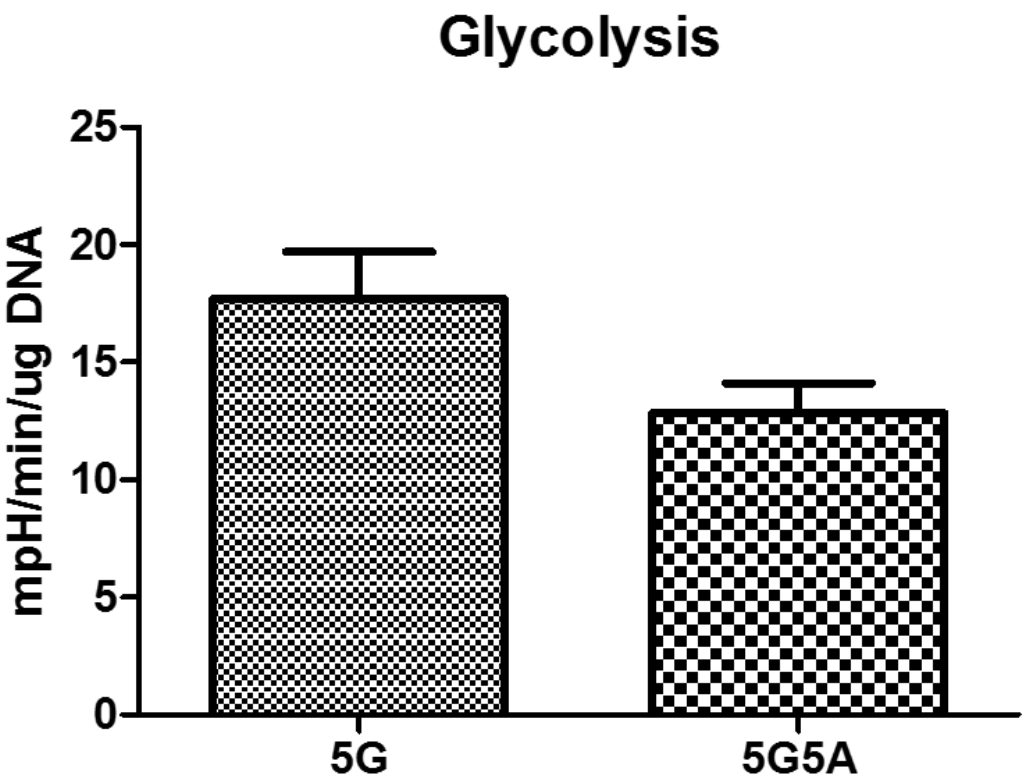
Glycolysis
mpH/min/ug DNA
25
20
15
10
5
0
5G
5G5A

Figure 21. Glycolytic Capacity for LLC-PK$_1$ cells grown in 5 mM acetoacetate. Cells cultured in 5 mM glucose(5G) or 5 mM glucose + 5 mM acetoacetate (5G5A) medium were assessed for glycolytic function via the Agilent-Seahorse Glyco ™ stress test once cells achieved 100% confluency and the Glyco Stress test protocol was used. The extracellular acidification rates (ECAR) were then recorded using the Seahorse Xfp analyzer (Agilent Technologies). Glycolytic capacity is (maximum rate measurement after oligomycin injection) – (last rate measurement before glucose injection). Statistical significance was determined using Student's unpaired t-test of five experiments. $P<0.05$(*)

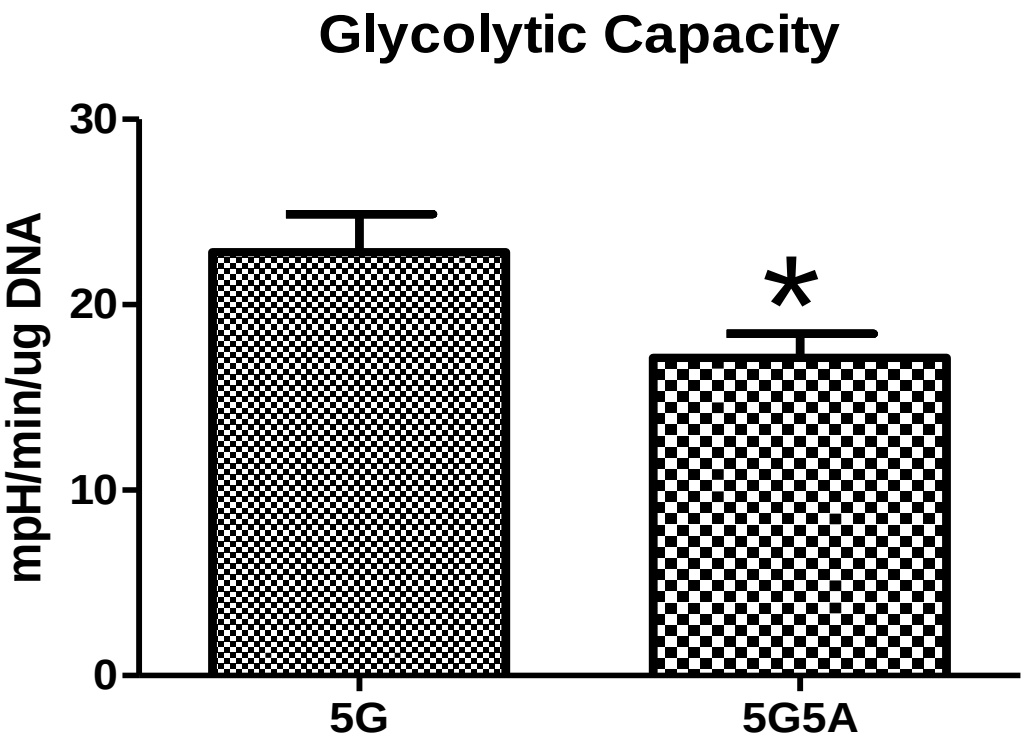
Glycolytic Capacity
mpH/min/ug DNA
30
20
10
0
*
5G
5G5A

Figure 22. Glycolytic Reserve for LLC-PK$_1$ cells grown in 5 mM acetoacetate. Cells cultured in 5 mM glucose (5G) or 5 mM glucose + 5 mM acetoacetate (5G5A) medium were assessed for glycolytic function via the Agilent-Seahorse Glyco ™ stress test once cells achieved 100% confluency and the Glyco Stress test protocol was used. The extracellular acidification rates (ECAR) were then recorded using the Seahorse Xfp analyzer (Agilent Technologies). Glycolytic reserve was calculated as (Glycolytic capacity) – (Glycolysis). Statistical significance was determined using Student's unpaired t-test of five experiments. $P<0.01$(**)

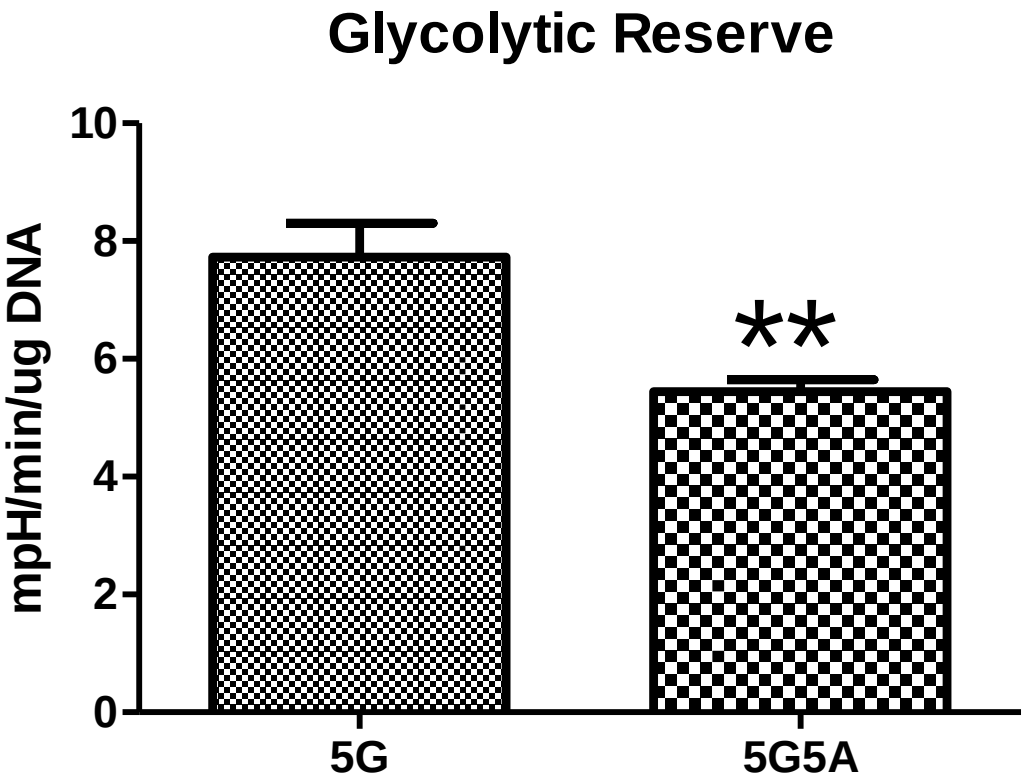
Glycolytic Reserve
mpH/min/ug DNA
10
8
6
4
2
0
**
5G
5G5A

Acetoacetate stimulated an increase in measured mitochondrial parameters, with a decrease in glycolytic capacity and glycolytic reserve. To determine if acetoacetate complemented media increases mitochondrial content, lysates of cells (20×10^6 cells) cultured in 5G or 5G5A media were assessed for citrate synthase activity, a marker of mitochondrial function and content (Larsen et al. 2012). There was a 44% increase in citrate synthase activity (figure 23) in cells cultured in the 5G5A medium (5G: 10.0 ± 0.78 nmol/min/mg protein, 5G5A: 14.4 ± 0.20 nmol/min/mg protein). This indicates that there is an increase in mitochondrial function and content.

To further determine mitochondrial content, biomarkers of mitochondrial biogenesis, PGC-1α (peroxisome-proliferator-activated receptor γ co-activator-1α) and TFAM (mitochondrial transcription factor A) were assessed in addition to mitochondrial protein COX IV. Acetoacetate complemented medium stimulated a 2.91-fold change in PGC-1α expression when compared to 5G (figure 24). There was a 2.41-fold change in TFAM (figure 25) and a 9.81-fold change in COX IV expression (figure 26) for cells cultured in 5G5A complemented medium. These results suggest that acetoacetate complemented media stimulated an increase in mitochondrial function and content.

Figure 23. Citrate Synthase activity for LLC-PK$_1$ cells grown in 5 mM acetoacetate. Cells cultured in 5 mM glucose (5G) or 5 mM glucose + 5 mM acetoacetate (5G5A) medium were lysed in RIPA buffer 100% confluency is achieved. Cells were then lysed using RIPA buffer and 5μL of lysates containing 5 μg of sample was used for the assay. Specific activity of citrate synthase (umols/min/mg) was determined via a plate based colorimetric measurement in accordance with the Cayman MitoCheck® Synthase Activity Assay kit. Statistical significance was determined using Student's unpaired t-test of four experiments. $P<0.01$(**)

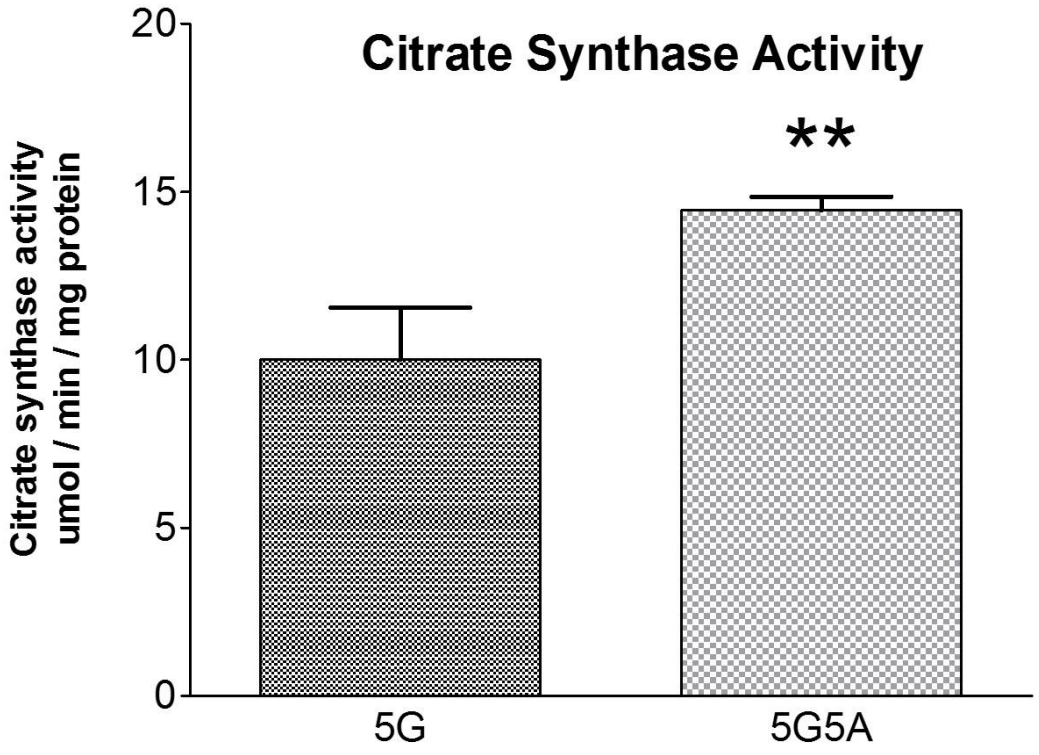
Citrate Synthase Activity
**
Citrate synthase activity
umol / min / mg protein
20
15
10
5
0
5G
5G5A

Figure 24. Expression of PGC-1α in LLC-PK$_1$ cells grown in 5 mM acetoacetate. Cells cultured in 5 mM glucose (5G) or 5 mM glucose + 5 mM acetoacetate (5G5A) medium were lysed in RIPA buffer 100% confluency is achieved. Cells were then lysed using RIPA buffer. Samples, at a concentration of 1 mg/ml were subjected to capillary electrophoresis followed by immunodetection. Expression of PGC-1α was normalized to expression of GAPDH. Statistical significance was determined using Student's unpaired t-test of four experiments. $P<0.05$(*)

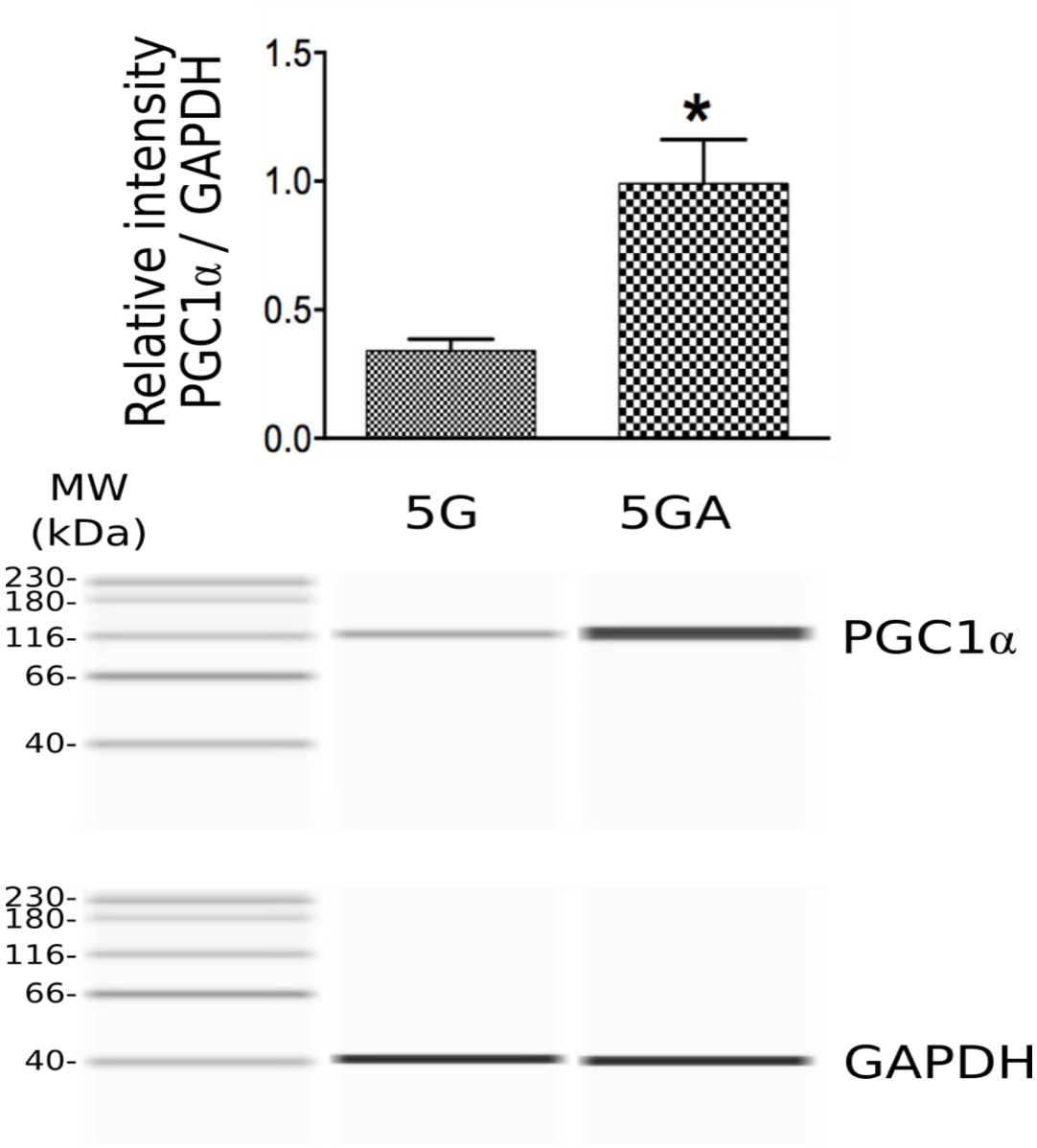
Relative intensity
PGC1α / GAPDH
1.5
1.0
0.5
0.0
*
MW
(kDa)
5G
5GA
230-
180-
116-
66-
40-
PGC1α
230-
180-
116-
66-
40-
GAPDH

Figure 25. Expression of TFAM in LLC-PK$_1$ cells grown in 5 mM acetoacetate. Cells cultured in 5 mM glucose (5G) or 5 mM glucose + 5 mM acetoacetate (5G5A) medium were lysed in RIPA buffer 100% confluency is achieved. Cells were then lysed using RIPA buffer. Samples, at a concentration of 1 mg/ml were subjected to capillary electrophoresis followed by immunodetection. Expression of TFAM was normalized to expression of GAPDH. Statistical significance was determined using Student's unpaired t-test of four experiments. $P<0.001$(***)

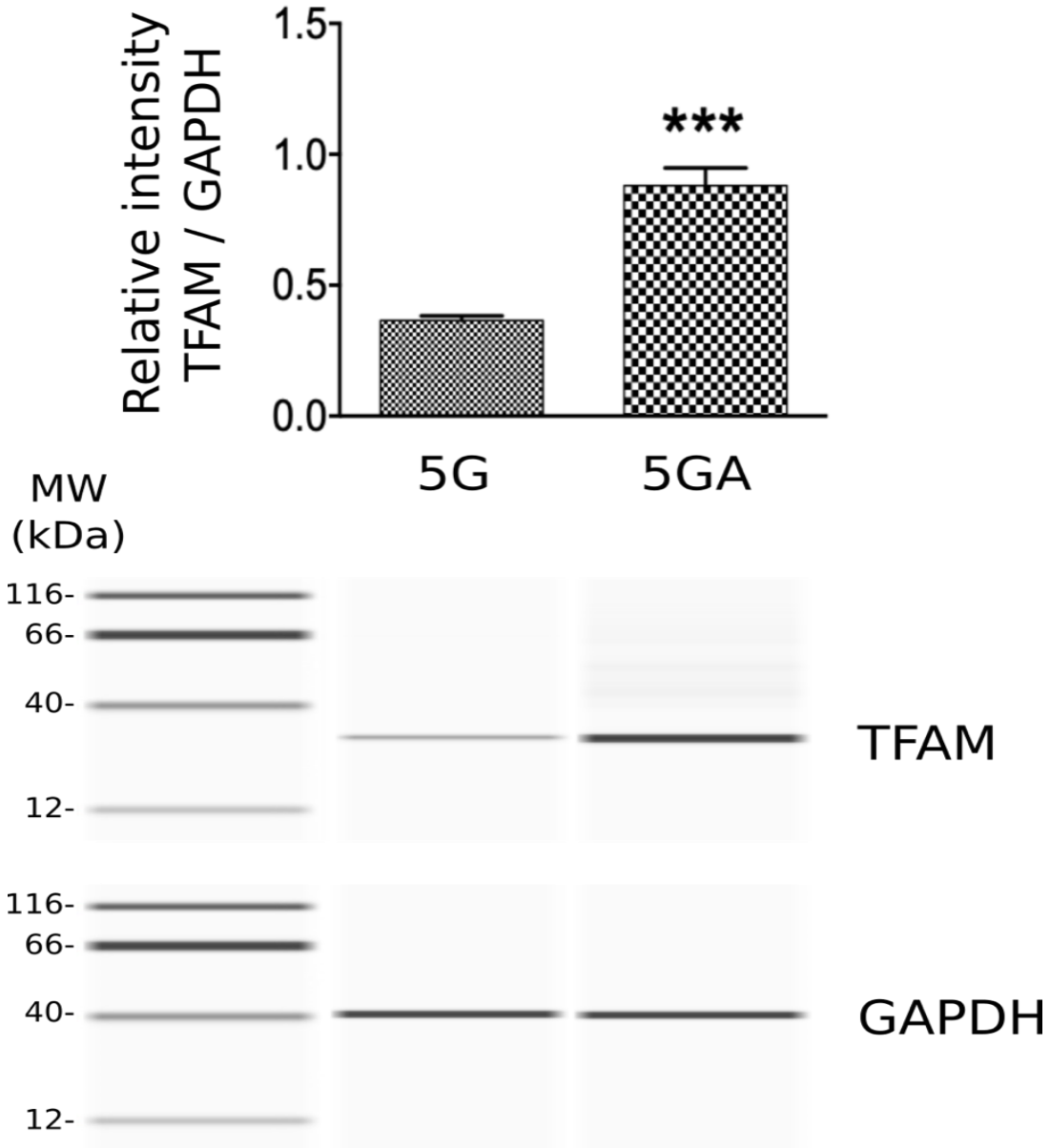
Relative intensity
TFAM / GAPDH
1.5
1.0
0.5
0.0
***
5G
5GA
MW
(kDa)
116-
66-
40-
12-
TFAM
116-
66-
40-
12-
GAPDH

Figure 26. Expression of COX IV in LLC-PK$_1$ cells grown in 5 mM acetoacetate. Cells cultured in 5 mM glucose (5G) or 5 mM glucose + 5 mM acetoacetate (5G5A) medium were lysed in RIPA buffer 100% confluency is achieved. Cells were then lysed using RIPA buffer. Samples, at a concentration of 1 mg/ml were subjected to capillary electrophoresis followed by immunodetection. Expression of COX IV was normalized to expression of GAPDH. Statistical significance was determined using Student's unpaired t-test of four experiments. $P<0.01$(**)

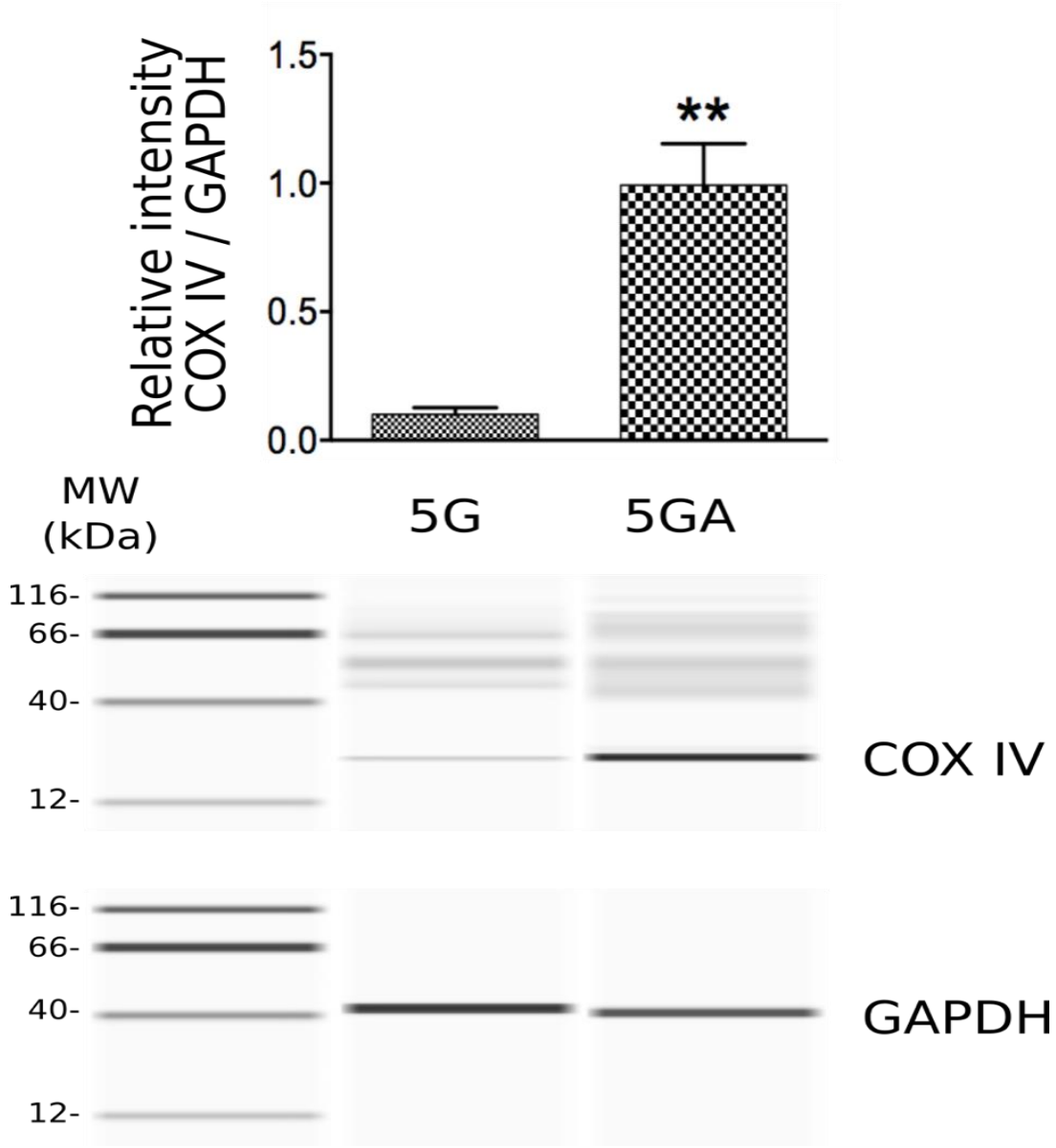
Relative intensity
COX IV / GAPDH
1.5
1.0
0.5
0.0
**
MW
(kDa)
5G
5GA
116-
66-
40-
12-
COX IV
116-
66-
40-
12-
GAPDH

Acetoacetate stimulated an increase in mitochondrial function and content. This increase may stimulate an increased sensitivity to mitochondrial toxicants. To examine if acetoacetate alters the LC_{50} value (table 1) of mitochondrial toxicants, a viability assay was conducted for 24 hours and viability assessed via a modified trypan blue assay (Hammoudeh et al. 2019). Cells cultured in 5G5A demonstrated a 36% decline in the LC_{50} value (713 ± 12 μM) when treated with diclofenac, a non-steroidal anti-inflammatory drug (NSAID), in comparison to 5G group (1112 ± 47 μM) (table 1). There was also a 19% decrease in the LC_{50} value (25.4 ± 0.95 μM) for cells cultured in 5G5A when treated with clotrimazole (antifungal agent), when compared to the LC_{50} value for 5G (31.2 ± 1.5 μM) (table 1). However, there were no significant differences in the LC_{50} values when cells in both media conditions were treated with ciprofibrate (anti-lipidemic agent) (table 1).

To assess if acetoacetate stimulates an increased response to mitochondrial toxicants, the Seahorse Mito ^{TM} stress test was conducted, and cells were exposed to the previously determined LC50 values of the mitochondrial toxicants. Diclofenac stimulated a 128% increase in OCR (Figure 27) for cells cultured in 5G5A (81.9 ± 6.1 pmol/min/μg DNA) when compared cells cultured in 5G only (36.0 ± 2.0 pmol/min/μg DNA). The increase in OCR post oligomycin was unaffected by the addition of FCCP, a known uncoupler, in both 5G and 5G5. This suggests that diclofenac acts an uncoupler. There was a significant decrease in OCR for both clotrimazole and ciprofibrate for cells in the 5G5A medium. Clotrimazole caused a 66% decline in OCR (figure 28) for cells cultured in 5G5A (56 ± 3.5 pmol/min/μg DNA) when compared to cells cultured in 5G only (33.7± 4.9 pmol/min/μg DNA).

Ciprofibrate treatment resulted in a 129% decrease in OCR (figure 29) for cells cultured in 5G5A (74.0 ± 3.7 pmol/min/µg DNA), when compared to the 5G group (32.3 ± 3.8 pmol/min/µg DNA). These compounds demonstrated a stronger inhibitory effect on the ETC (electron transport) chain in the 5G5A group. These findings indicate that acetoacetate complemented media can sensitize cells to mitochondrial toxicants, improving the model for toxicity screening.

Table 5. LC_{50} value for mitochondrial toxicants in LLC-PK_1 cells grown in 5 mM acetoacetate. Cells cultured in 5 mM glucose (5G) or 5 mM glucose + 5 mM acetoacetate (5G5A) medium were seeded in 96 well plates at a density of 15 X 10^3 cells/well and allowed to grow until confluent monolayers were formed. Cells were then treated for 24 hours with increasing concentrations of diclofenac (0.5 - 5mM), clotrimazole (0.1 – 100 µM) and ciprofibrate (1 - 40 µM). Cell viability measured using a modified trypan blue-based viability assessment (Hammoudeh et al. 2019). Statistical significance was determined using Student's unpaired t-test of four experiments $p<0.05$(*)

Compound	**LC_{50} value 5G**	**LC_{50} value 5G5A**
Diclofenac	1112± 46.98 μM	713 ± 11.99 μM *
Clotrimazole	31.18 ± 1.47 μM	25.41 ± 0.95 μM *
Ciprofibrate	18.34 ± 3.06 μM	26.14 ± 4.73 μM

Figure 27. Acute response of LLC-PK$_1$ cells to the LC $_{50}$ value of Diclofenac. LLC-PK$_1$ cells were seeded into an 8 well extracellular flux mini culture plate at a density of 8×10^4 cells/well. The cells were cultured in either 5 mM glucose (5G) or 5 mM glucose + 5 mM acetoacetate (5G5A) for 48 hours to achieve confluency and a modified Agilent-Seahorse Mito Stress test protocol was used. Cells were exposed to 1μM Oligomycin, followed by the previously determined LC_{50} value of diclofenac for 5G (1112 μM) or 5G5A (713.3μM). This was then followed by 1μM of FCCP and finally a mixture of rotenone and antimycin A at 0.5 μM. The oxygen consumption rates (OCR) were then recorded using the Seahorse Xfp analyzer. Maximal respiration was calculated as maximum rate measurement after FCCP injection) - (non-mitochondrial respiration). Statistical significance was determined using Student's unpaired t-test of five experiments. P<0.001(***)

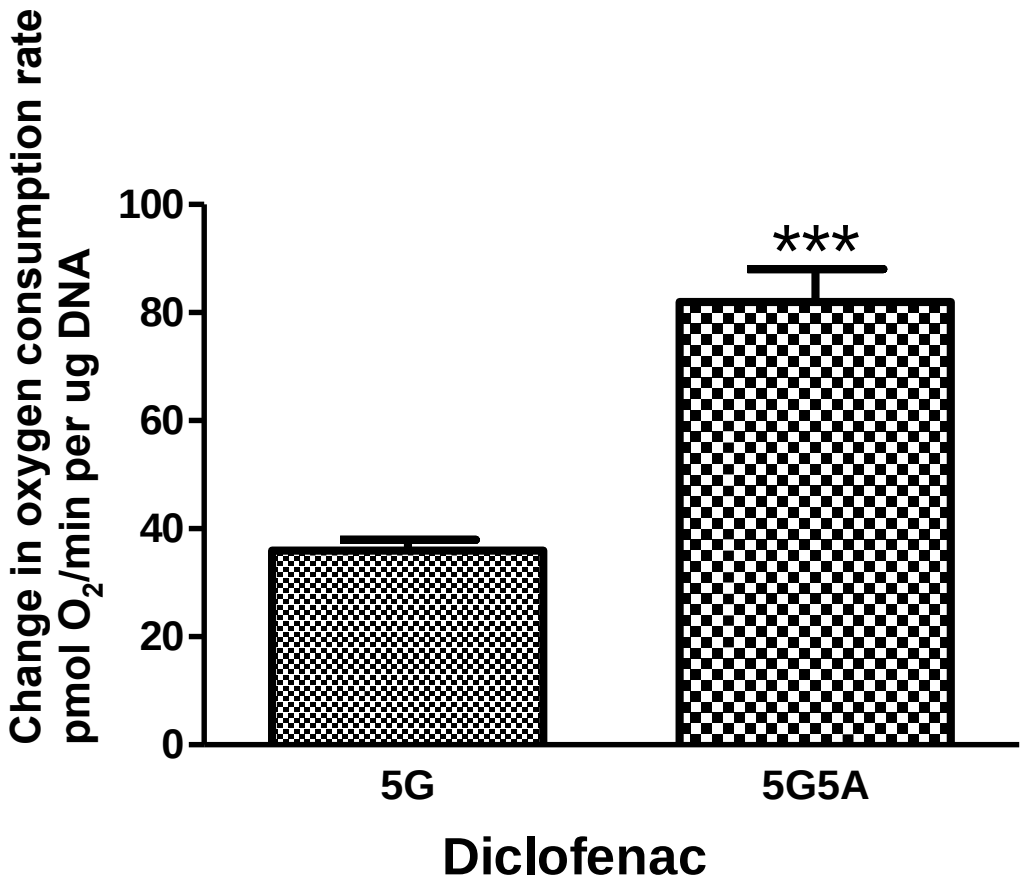
Change in oxygen consumption rate
pmol O2/min per ug DNA
100
80
60
40
20
0
***
5G
5G5A
Diclofenac

Figure 28. Acute response of LLC-PK$_1$ cells to the LC $_{50}$ value of Clotrimazole. LLC-PK$_1$ cells were seeded into an 8 well extracellular flux mini culture plate at a density of 8×10^4 cells/well. The cells were cultured in either 5 mM glucose (5G) or 5 mM glucose + 5 mM acetoacetate (5G5A) for 48 hours to achieve confluency and the Agilent-Seahorse Mito Stress test protocol was then used. The oxygen consumption rates (OCR) were then recorded using the Seahorse Xfp analyzer. Cells were exposed to the LC_{50} value of clotrimazole for 5G (31.2µM) or 5G5A (25.4 µM). Decrease in Oxygen consumption rate (OCR) was calculated by subtracting maximal OCR post FCCP – lowest OCR post clotrimazole. Statistical significance was determined using Student's unpaired t-test of five experiments. $P<0.05$(*)

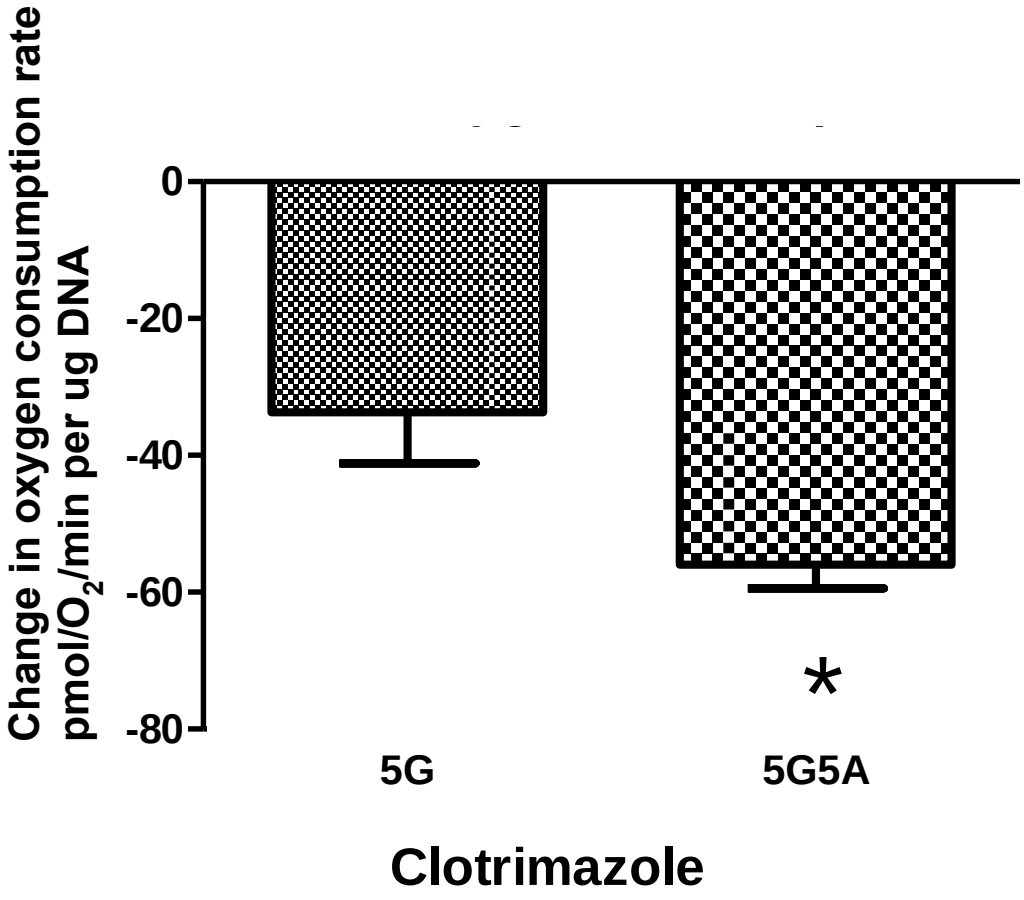
Change in oxygen consumption rate
pmol/O2/min per ug DNA
0
-20
-40
-60
-80
*
5G
5G5A
Clotrimazole

Figure 29. Acute response of LLC-PK$_1$ cells to the LC $_{50}$ value of Ciprofibrate. LLC-PK$_1$ cells were seeded into an 8 well extracellular flux mini culture plate at a density of 8×10^4 cells/well. The cells were cultured in either 5 mM glucose (5G) or 5 mM glucose + 5 mM acetoacetate (5G5A) for 48 hours to achieve confluency and the Agilent-Seahorse Mito Stress test protocol was then used. The oxygen consumption rates (OCR) were then recorded using the Seahorse Xfp analyzer. Cells were exposed to the LC_{50} value of ciprofibrate for 5G (18.3 μM) and 5G5A (26.1μM). Decrease in Oxygen consumption rate (OCR) was calculated by subtracting maximal OCR post FCCP – lowest OCR post clotrimazole. Statistical significance was determined using Student's unpaired t-test of five experiments. P<0.001(***)

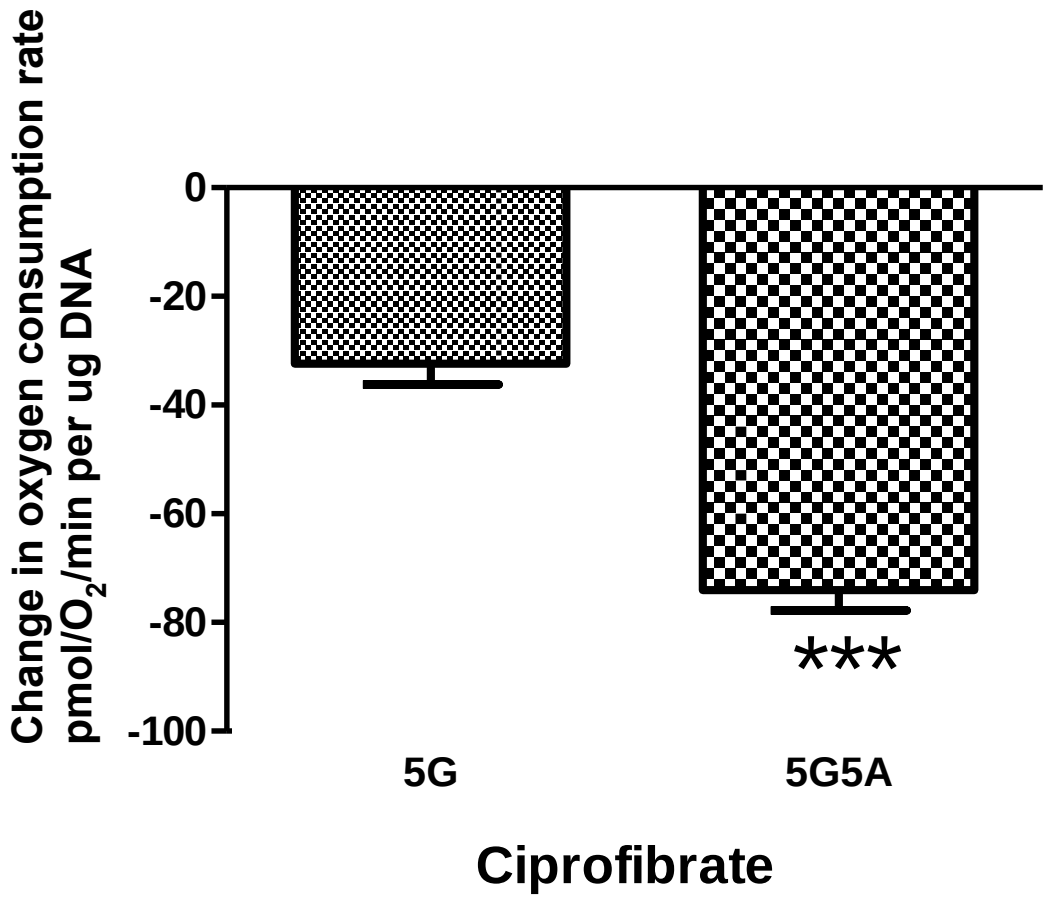
Change in oxygen consumption rate
pmol/O2/min per ug DNA
0
-20
-40
-60
-80
-100
***
5G
5G5A
Ciprofibrate

4. DISCUSSION

The results of this study have demonstrated that culture media complemented with acetoacetate, can induce a change in the bioenergetic profile of LLC-PK_1 cells, resulting in a cell line with increased sensitivity to mitochondrial toxicants. Lowering the glucose concentration from 17.5 mM to 5 mM, did not alter the mitochondrial function (figure 5- figure 8). A reduced glucose concentration also failed to reduce glycolytic function (figure 9-figure 11). Quercetin did not alter mitochondrial function. Although previously mentioned studies indicated that quercetin can increase mitochondrial function, that was not observed in our study. Quercetin inhibited cell proliferation in human breast carcinoma SK-Br3 cells, in a dose dependent manner (1 μM to 10 μM) (Jeong et al. 2009). Quercetin did not impact cell proliferation for LLC-PK_1 cells at 15 μM, however, the impact of quercetin on mitochondrial function has not yet been determined and will be evaluated in future studies. Extracellular flux analysis demonstrated that acetoacetate stimulated an increase in mitochondrial function, accompanied by a decrease in glycolytic capacity and reserve.

Additionally, acetoacetate stimulated an increase in citrate synthase activity, as well as an increase in PGC-1α, TFAM and COX IV protein expression. This indicates that this cell line was genetically reprogrammed by the presence of acetoacetate in the culture media. It is well known the acetoacetate can be utilized as a source of fuel. Additionally, acetoacetate as well as betahydroxybutyrate can participate in signaling pathways that result in a change in metabolic activity (Grabacka et al. 2016). Therefore, this ketone body can affect mitochondrial and glycolytic function via any of the above-mentioned mechanisms.

Acetoacetate stimulated an increase in basal respiration. Basal respiration is the baseline oxygen consumption that is controlled by ATP turnover, substrate oxidation and proton leak. Basal respiration is sensitive to changes in ATP demand or the presence of different substrates (Brand and Nicholls 2011). The addition and oxidation of fatty acids and pyruvate can greatly increase the basal respiration rates of hepatocytes (Brand and Nicholls 2011). Likewise, the addition of acetoacetate stimulated an increase in LLC-PK_1 cells. ATP turnover is the ratio between ATP production and ATP content. (Brand and Nicholls 2011). Increase in ATP utilization will affect ATP content and stimulate and increase in ATP production. This will then increase basal respiration. ATP linked respiration can be described as the rate of mitochondrial ATP synthesis in a basal state (Brand and Nicholls 2011). Substrate oxidation can influence ATP turnover, resulting in an increase in ATP production. As a result, ATP linked respiration was significantly increased in the acetoacetate group.

Uncoupled respiration (maximal respiration) was significantly higher in cells that were cultured in the presence of acetoacetate. The rate of respiration is controlled by two factors, the mitochondrial proton circuit and the thermodynamic disequilibrium. In the mitochondrial proton circuit, proton extrusion balances proton reentry under steady state conditions (Brand and Nicholls 2011). Additionally, the rate of respiration also requires a thermodynamic disequilibrium, where the free energy required for electron transfer must be greater than energy required to pump protons across the membrane against the protonmotive force (PMF) (Brand and Nicholls 2011). This disequilibrium is necessary for the forward movement of electrons through the different complexes. Therefore, FCCP stimulates increase in

respiration by inducing an artificial proton permeability in the mitochondrial membrane. This lowers PMF and increases the thermodynamic disequilibrium, which is a factor that controls respiration (Brand and Nicholls 2011). As a result, the proton current and respiration increases. Reduced or low maximal respiration values can indicate mitochondrial dysfunction. The significant increase in maximal respiration indicates a significant increase in spare respiratory capacity, which is the difference between maximal and basal respiration.

The spare respiratory capacity is the ability of the substrate supply and electron transport to respond to an increase in energetic demand (Brand and Nicholls 2011). An energetic demand is created when an energy pathway is inhibited and the cells must rely on another pathway to maintain ATP content. A reduced or small respiratory capacity can indicate mitochondrial dysfunction that is often not apparent under basal or baseline cellular conditions (Brand and Nicholls 2011). Thus, it can be safely assumed that the addition of acetoacetate had a significant effect on mitochondrial activity.

The results of this study indicate that acetoacetate complemented media, increased PGC-1α expression which resulted in an increase in mitochondrial content. PGC-1α [PPAR (peroxisome proliferator-activated receptor)-γ coactivator-1α] is often viewed as a master regulator of mitochondrial biogenesis (Jornayvaz and Shulman 2010). An increase in PGC-1α mRNA expression in skeletal muscle and brown fat, was accompanied by an increased expression of mitochondrial proteins namely ATP synthase (β subunit) and Cytochrome c oxidase (COXIV) subunits (Puigserver et al. 1998). PGC-1α regulates mitochondrial biogenesis by activating the

transcription factors nuclear respiratory factors 1 and 2 (NRF1 and NRF2) which stimulate expression of mitochondrial transcription factor A (TFAM) (Jornayvaz and Shulman 2010). NRF-1 and 2 are activated downstream of PGC1α where they regulate genes associated with mitochondrial respiration (Scarpulla, 2011). NRF-1 targets are genes that encode the subunits of the five complexes (Scarpulla 2006). NRF-1 also increases the expression of human genes encoding constituents of the mtDNA transcription machinery which are nuclear encoded factors that control mitochondrial gene expression (Scarpulla 2006).

They include TFAM, TFB1M, TFB2M (transcription specificity factors B1 and B2 mitochondrial), and POLRMT (mitochondrial RNA polymerase) (Scarpulla, 2006). NRF-1 binds to the promoter regions of TFAM and TFB1M and TFB2M, increasing mitochondrial transcription (Scarpulla, 2008). Additionally, NRF-2 also binds to the above-mentioned transcription factors as well as the cis elements in the promoter region of COXIV (Scarpulla 2008).

Based on the results, acetoacetate can stimulate increase in mitochondrial content in a PGC-1α mediated manner, resulting in an increased protein expression of TFAM and COX IV. This was further supported by an increase in citrate synthase activity (Figure 19). Transmission electron microscopy of skeletal muscle revealed a strong correlation between mitochondrial fractional area and citrate synthase activity (Larsen et al. 2012). Despite these findings, the exact signaling pathway by which acetoacetate stimulates an increase in function and content in not yet known. Acetoacetate can also be used as a source of considerable energy, which can meet the

energy demands of transporting epithelia such as proximal tubular cells (Cotter et al.2013).

Acetoacetate undergoes ketolysis, which is the oxidation of acetoacetate to yield acetyl CoA during times of starvation and increased energy demand (Gabacka et al. 2016). It is a pathway that take place in the mitochondria of most cells except hepatocytes and most malignantly transformed cells (Grabacka et al. 2016). LLC PK_1 cells are non-malignantly transformed and can utilize acetoacetate in this manner.

Oxidation of acetoacetate which yields two molecules of acetyl CoA can result in an increase in citrate levels that can potentially impact glycolytic activity. Citrate inhibits phosphofructokinase, the regulatory enzyme of glycolysis (Usenik and Legisa, 2010). Results of this study demonstrate a reduction in glycolytic capacity as well as glycolytic reserve. Glycolytic capacity is a measure of the cell's maximum conversion rate of glucose to pyruvate or lactate (Mookerjee et al. 2016). It is a measure of the maximum capacity to generate ATP via glycolysis given that glycolytic ATP synthesis is linked to glycolytic carbon flux (Mookerjee et al. 2016). This maximum increase is measured in the presence of added glucose, and oligomycin, which inhibits ATP synthase. A reduced glycolytic capacity demonstrates a limited glycolytic machinery (Mookerjee et al. 2016).

Glycolytic reserve indicates how well the cell can respond to an energetic demand using glycolysis. This parameter was significantly lower for cells grown in the presence of acetoacetate, suggesting that their ability to utilize glycolysis is reduced. The exact mechanism that illustrates the effect acetoacetate has on the glycolytic activity of LLC-PK_1 cells is not yet known.

The results of this study indicate that acetoacetate has reprogrammed the LLC-PK$_1$ cell line in PGC-1α mediated manner. However, the exact mechanism has not been examined in this study. A possible mechanism is the histone deacetylase (HDAC) inhibition pathway. HDAC are enzymes that remove an acetyl group from histones which are proteins that package and compact chromosomal DNA into the nucleus, resulting in a DNA/protein complex that is chromatin (Mihaylova and Shaw, 2013). In this form, DNA is less accessible to transcription factors. Thus, HDACs have a repressive effect on transcription (Mihaylova et al. 2013). HDAC inhibitors inhibit the action of these enzymes facilitating transcription of genes that regulate energy metabolism (Mihaylova et al. 2013). Betahydroxybutyrate (BHB), has been shown to act as a class I HDAC inhibitor (Shimazu et al. 2013). BHB stimulated global acetylation via inhibition of HDAC in human embryonic kidney cells (HEK 293) when treated with BHB for 8 hours at 1, 2, and 3 mM concentrations (Shimazu et al. 2013).

Additionally, HDAC inhibitors such as valproic acid have been shown to inhibit glucose transport and hexokinase 1 activity in the OPM2 human multiple myeloma cell line (Wardell et al. 2009). Valproic acid also upregulated PGC-1α expression in SH-SY5Y neuroblastoma cells at 10 mM at 48hrs (Cowell et al. 2009). It is possible that acetoacetate acts an HDAC inhibitor, stimulating an increase in PGC-1α expression.

A reduction of glycolytic capacity and reserve coupled with an increase in mitochondrial function represents a shift in energy metabolism resulting in a model

with increased sensitivity to mitochondrial toxicants. Diclofenac stimulated a significant increase in OCR in the acetoacetate group, indicating that this NSAID acts as an uncoupler (Moreno-Sanchez et al. 1999). This increased sensitivity to mitochondrial toxicants is due to the reduced glycolytic function combined with an increased reliance on oxidative phosphorylation. The cells are unable to utilize glycolysis sufficiently when mitochondrial function is compromised.

Clotrimazole and ciprofibrate have been documented as ETC inhibitors (Wills et al. 2015). ETC inhibitors decrease OCR. The results of this study have shown that the toxic effects of clotrimazole and ciprofibrate were more pronounced in the cells grown in the acetoacetate complemented medium. This indicates that acetoacetate increased the sensitivity of LLC-PK_1 cells to toxicants. Although the LC_{50} value for ciprofibrate did not decrease significantly for cells grown in acetoacetate, there was a significant decrease in OCR for the acetoacetate group when treated with ciprofibrate. The results suggest that viability assays alone are not representative of mitochondrial toxicity.

In conclusion, addition of acetoacetate to culture media resulted in an increase in mitochondrial function and content, with a concomitant reduction in glycolytic capacity and reserve. This shift in energy metabolism results in a model with increased sensitivity to toxicants, improving its sensitivity and reliance as a model for toxicity screening and testing.

5. FUTURE DIRECTIONS

Further studies will elucidate the signaling pathway that results in an increase in mitochondrial function and content. Assessment of HDAC activity can elucidate the impact of acetoacetate on PGC-1α expression. HDAC inhibition will result in increased acetylation of histone proteins (Shimazu et al. 2013). Analysis of acetylated histone levels in the presence of acetoacetate can elucidate a potential mechanism that stimulates an increase in mitochondrial biogenesis.

It is necessary to compare the improved sensitivity of LLC-PK_1 cells with other routinely used cell lines such as HK-2, HEK 293 and the primary proximal tubular cultures. Comparative viability assays will determine if acetoacetate confers greater sensitivity to LLC-PK_1 cells than the immortalized human cell lines and the primary counterparts. Additionally, future studies will determine if acetoacetate complemented media can reprogram the above-mentioned immortalized cell lines by stimulating an increase in mitochondrial function with a concomitant increase in sensitivity to mitochondrial toxicants.

The purpose of this study was to improve renal culture cells for *in vitro* toxicity testing. It is necessary to examine the efficacy of acetoacetate complemented media in a high throughput screening platform. This will facilitate screening of multiple pharmacologically relevant compounds for nephrotoxicity and will demonstrate the improved sensitivity of this culture method.

6. APPENDIX

Media Composition: SFFD (DMEM: Ham's F-12)

COMPONENTS	**MW**	**SFFD**	
Catalog number			
Amino Acids		**mg/L**	**mM**
Glycine	75	18.75	0.25
L-Alanine	89	4.45	0.05
L-Arginine hydrochloride	211	147.5	0.699
L-Asparagine-H2O	150	7.5	0.05
L-Aspartic acid	133	6.65	0.05
L-Cysteine hydrochloride-H2O	176	17.56	0.0998
L-Cystine 2HCl	313	31.29	0.1
L-Glutamic Acid	147	7.35	0.05
L-Glutamine	146	365	2.5
L-Histidine hydrochloride-H2O	210	31.48	0.15
L-Isoleucine	131	54.47	0.416
L-Leucine	131	59.05	0.451
L-Lysine hydrochloride	183	91.25	0.499
L-Methionine	149	17.24	0.116
L-Phenylalanine	165	35.48	0.215
L-Proline	115	17.25	0.15
L-Serine	105	26.25	0.25
L-Threonine	119	53.45	0.449
L-Tryptophan	204	9.02	0.0442
L-Tyrosine	181		
L-Tyrosine disodium salt dihydrate	261	55.79	0.214
L-Valine	117	52.85	0.452

6. APPENDIX

Media Composition

COMPONENTS	MW	SFFD	
Vitamins		**mg/mL**	
Biotin	244	0.0035	0.0000143
Choline chloride	140	8.98	0.0641
D-Calcium pantothenate	477	2.24	0.0047
Folic Acid	441	2.65	0.00601
i-Inositol	180	12.6	0.07
Niacinamide	122	2.02	0.0166
Pyridoxine hydrochloride	206	2	0.00971
Riboflavin	376	0.219	0.000582
Thiamine hydrochloride	337	2.17	0.00644
Vitamin B12	1355	0.68	0.000502

6. APPENDIX

Inorganic Salts	MW	Mg/mL	mM
Calcium Chloride (CaCl2) (anhyd.)	111	116.6	1.05
Cupric sulfate (CuSO4-5H2O)	250	0.0013	0.0000052
Ferric Nitrate (Fe(NO3)3"9H2O)	404	0.05	0.000124
Ferric sulfate (FeSO4-7H2O)	278	0.417	0.0015
Magnesium Chloride (anhydrous)	95	28.64	0.301
Magnesium Sulfate (MgSO4) (anhyd.)	120	48.84	0.407
Potassium Chloride (KCl)	75	311.8	4.16
Sodium Bicarbonate (NaHCO3)	84	1200	14.29
Sodium Chloride (NaCl)	58	6995.5	120.61
Sodium Phosphate dibasic (Na2HPO4) anhydrous	142	71.02	0.5
Sodium Phosphate monobasic (NaH2PO4-H2O)	138	62.5	0.453
Zinc sulfate (ZnSO4-7H2O)	288	0.432	0.0015

6. APPENDIX

Other Components	MW	mg/mL	mM
D-Glucose (Dextrose)	180	3151	17.51
HEPES	238	3574.5	15.02
Hypoxanthine Na	159	2.39	0.015
Linoleic Acid	280	0.042	0.00015
Lipoic Acid	206	0.105	0.00051
Phenol Red	376.4	8.1	0.0215
Putrescine 2HCl	161	0.081	0.000503
Sodium Pyruvate	110	55	0.5
Thymidine	242	0.365	

Citrate Synthase Activity

Working Reagent Preparation

Reagent A	Reagent B
20 µL of Acetyl coA reagent	20 µL of Oxaloacetate reagent
20 µL of Developer reagent	480 µL of Assay buffer
960 µL of Assay buffer	

7. BIBLIOGRAPHY

Andreux, P. A., Mouchiroud, L., Wang, X., Jovaisaite, V., Mottis, A., Bichet, S., Auwerx, J. (2014). A Method to Identify and Validate Mitochondrial Modulators using Mammalian Cells and the Worm C. Elegans. *Scientific reports*, 4, 5285. doi:10.1038/srep05285

Bonventre, J. V., Vaidya, V. S., Schmouder, R., Feig, P., & Dieterle, F. (2010). Next-Generation Biomarkers for Detecting Kidney Toxicity. *Nature biotechnology*, 28(5), 436–440. doi:10.1038/nbt0510-436

Brand, M. D., & Nicholls, D. G. (2011). Assessing Mitochondrial Dysfunction in Cells. *The Biochemical journal*, 435(2), 297–312. doi:10.1042/BJ20110162

Cotter, D. G., Schugar, R. C., & Crawford, P. A. (2013). Ketone Body Metabolism and Cardiovascular Disease. *American journal of physiology*. Heart and circulatory physiology, 304(8), H1060–H1076. doi:10.1152/ajpheart.00646.2012

Cowell, R. M., Talati, P., Blake, K. R., Meador-Woodruff, J. H., & Russell, J. W. (2009). Identification of Novel Targets for PGC-1α and Histone Deacetylase Inhibitors in Neuroblastoma Cells. *Biochemical and biophysical research communications*, 379(2), 578–582. doi:10.1016/j.bbrc.2008.12.109

Davila, J. C., Rodriguez, R. J., Melchert, R. B., & Acosta, D. (1998). Predictive Value of *In Vitro* Model Systems in Toxicology. *Annual Review of Pharmacology and Toxicology*, 38(1), 63–96. doi.org/10.1146/annurev.pharmtox.38.1.63

Díaz-Ruiz, R., Avéret, N., Araiza, D., Pinson, B., Uribe-Carvajal, S., Devin, A., & Rigoulet, M. (2008). Mitochondrial Oxidative Phosphorylation is Regulated by Fructose 1,6-Bisphosphate. *Journal of Biological Chemistry*, 283(40), 26948–26955. doi: 10.1074/jbc.M800408200

Felder, E., Jennings, P., Seppi, T., & Pfaller, W. (2002). LLC-PK 1 Cells Maintained in a New Perfusion Cell Culture System Exhibit an Improved Oxidative Metabolism. *Cellular Physiology and Biochemistry*, (12) 153–162. doi.org/10.1159/000063792

George, B., You, D., Joy, M. S., & Aleksunes, L. M. (2017). Xenobiotic Transporters and Kidney Injury. *Advanced drug delivery reviews*, *116*, 73–91. doi:10.1016/j.addr.2017.01.005

Grabacka, M., Pierzchalska, M., Dean, M., & Reiss, K. (2016). Regulation of Ketone Body Metabolism and the Role of PPARα. *International journal of molecular sciences, 17*(12), 2093. doi:10.3390/ijms17122093

Gstraunthaler, G., Seppi, T., & Pfaller, W. (1999). Impact of Culture Conditions, Culture Media Volumes, and Glucose Content on Metabolic Properties of Renal Epithelial Cell Cultures. *Cellular Physiology and Biochemistry*, 9(3), 150–172. doi: 10.1159/000016312

Hammoudeh, S. M., Hammoudeh, A. M., & Hamoudi, R. (2019). High-Throughput Quantification of the Effect of DMSO on the Viability of Lung and Breast Cancer Cells using an Easy-to-use Spectrophotometric Trypan Blue-Based Assay. *Histochemistry and Cell Biology*, 152(1), 75–84. doi:10.1007/s00418-019-01775-7

Heussner, A. H., & Dietrich, D. R. (2013). Primary Porcine Proximal Tubular Cells as an Alternative to Human Primary Renal Cells *In Vitro*: An Initial Characterization. *BMC cell biology,* 14, 55. doi:10.1186/1471-2121-14-55

Hull, R., Cherry, W., & Weaver, G. (1976). The origin and characteristics of a pig kidney cell strain, LLC-PK. *In Vitro Cellular & Developmental Biology – Plant* 12(10), 670-677. doi:10.1007/BF02797469

Jeong, J. H., An, J. Y., Kwon, Y. T., Rhee, J. G., & Lee, Y. J. (2009). Effects of Low Dose Quercetin: Cancer Cell-Specific Inhibition of Cell Cycle Progression. *Journal of cellular biochemistry*, 106(1), 73–82. doi:10.1002/jcb.21977

Jornayvaz, F. R., & Shulman, G. I. (2010). Regulation of Mitochondrial Biogenesis. *Essays in Biochemistry,* 47, 69–84. doi:10.1042/bse0470069

Kim, C. S., Kwon, Y., Choe, S. Y., Hong, S. M., Yoo, H., Goto, T., Kawada, T., Choi, H., Joe, Y., Chung, H.T., & Yu, R. (2015). Quercetin Reduces Obesity-Induced Hepatosteatosis by Enhancing Mitochondrial Oxidative Metabolism via Heme Oxygenase-1. *Nutrition & metabolism*, 12, 33. doi:10.1186/s12986-015-0030-5

Konopka, A. R., Suer, M. K., Wolff, C. A., & Harber, M. P. (2014). Markers of Human Skeletal Muscle Mitochondrial Biogenesis and Quality Control: Effects of Age and Aerobic Exercise Training. *The journals of gerontology. Series A, Biological sciences and medical sciences*, 69(4), 371–378. doi:10.1093/gerona/glt107

Larsen, S., Nielsen, J., Hansen, C. N., Nielsen, L. B., Wibrand, F., Stride, N., Schroder, H.D., Boushel, R., Helge, J.W., Dela, F., & Hey-Mogensen, M. (2012). Biomarkers of Mitochondrial Content in Kkeletal Muscle of Healthy

Young Human Subjects. *The Journal of physiology*, 590(14), 3349–3360. doi:10.1113/jphysiol.2012.230185

Li, W., Choy, D. F., Lam, M. S., Morgan, T., Sullivan, M. E., & Post, J. M. (2003). Use of Cultured Cells of Kidney Origin to Assess Specific Cytotoxic Effects of Nephrotoxins. *Toxicology In Vitro*, 17(1), 107–113. https://doi.org/10.1016/S0887-2333(02)00128-5

Li, Y., Oo, Z. Y., Chang, S. Y., Huang, P., Eng, K. G., Zeng, J. L., Zink, D. (2013). An in vitro method for the prediction of renal proximal tubular toxicity in humans. *Toxicology Research*, 2(5), 352–365. doi: 10.1039/C3TX50042J

Lim, J. H., Gerhart-Hines, Z., Dominy, J. E., Lee, Y., Kim, S., Tabata, M., Xiang, Y.K., & Puigserver, P. (2013). Oleic Acid Stimulates Complete Oxidation of Fatty Acids through Protein Kinase A-dependent Activation of SIRT1-PGC1α Complex. *The Journal of biological chemistry*, 288(10), 7117–7126. doi:10.1074/jbc.M112.415729

Lohr, J. W., Willsky, G. R., & Acara, M. A. (1998). Renal Drug Metabolism. *Pharmacological Reviews*, 50(1), 107–141. doi:0031-6997/98/5001-0107

Mandel, L. J. (1986). Primary Active Sodium Transport, Oxygen Consumption, and ATP: Coupling and Regulation. *Kidney international*, 29(1), 3–9. doi:10.1038/ki.1986.2

Marroquin, L. D., Hynes, J., Dykens, J. A., Jamieson, J. D., & Will, Y. (2007). Circumventing the Crabtree Effect: Replacing Media Glucose with Galactose Increases Susceptibility of HepG2 Cells to Mitochondrial Toxicants. *Toxicological sciences*, 97(2), 539–547 doi:10.1093/toxsci/kfm052

Mihaylova, M. M., & Shaw, R. J. (2013). Metabolic Reprogramming by Class I and II Histone Deacetylases. *Trends in Endocrinology and Metabolism*, 24(1), 48–57. doi:10.1016/j.tem.2012.09.003

Mookerjee, S. A., Nicholls, D. G., & Brand, M. D. (2016). Determining Maximum Glycolytic Capacity Using Extracellular Flux Measurements. *PloS one*, 11(3), e0152016. doi:10.1371/journal.pone.0152016

Moreno-Sanchez, R., Silveira, L. H., & Martınez, M. (1999). Inhibition and Uncoupling of Oxidative Phosphorylation by Nonsteroidal Anti-Inflammatory Drugs. *Biochemical pharmacology* 57(98), 743–752. doi:10.1016/s0006-2952(98)00330-x

Nourbakhsh, N., & Singh, P. (2014). Role of renal oxygenation and mitochondrial function in the pathophysiology of acute kidney injury. *Nephron. Clinical practice*, 127(1-4), 149–152. doi:10.1159/000363545

Nowak, G., & Schnellmann, R. G. (1995). Improved Culture Conditions Stimulate Gluconeogenesis in Primary Cultures of Renal Proximal Tubule Cells. *American journal of physiology-Cell physiology*, 268(4), C1053–C1061. doi: 10.1152/ajpcell.1995.268.4.c1053

Nowak, G., & Schnellmann, R. G. (1996). L-ascorbic Acid Regulates Growth and Metabolism of Renal Cells: Improvements in Cell Culture. *American journal of physiology-Cell physiology*, 271(6), C2072–C2080. doi:10.1152/ajpcell.1996.271.6.c2072

Puigserver, P., Wu, Z., Park, C. W., Graves, R., Wright, M., & Spiegelman, B. M. (1998). A cold-inducible coactivator of nuclear receptors linked to adaptive thermogenesis. Cell, 92(6), 829–839. doi.org:10.1016/S0092-8674(00)81410-5

Rana, P., Aleo, M. D., Gosink, M., & Will, Y. (2019). Evaluation of in Vitro Mitochondrial Toxicity Assays and Physicochemical Properties for Prediction of Organ Toxicity Using 228 Pharmaceutical Drugs. *Chemical research in toxicology*, 32(1), 156–167. doi:10.1021/acs.chemrestox.8b00246

Rayamajhi, N., Kim, S. K., Go, H., Joe, Y., Callaway, Z., Kang, J. G., Ryter, S.W., Chung, H. T. (2013). Quercetin Induces Mitochondrial Biogenesis Through Activation of HO-1 in HepG2 Cells. *Oxidative medicine and cellular longevity, 2013*, 154279. doi:10.1155/2013/154279

Rodriguez-Enriquez, S., Juarez, O., Rodriguez-Zavala, J. S., & Moreno-Sanchez, R. (2001). Multisite Control of the Crabtree Effect in Ascites Hepatoma Cells. *European journal of biochemistry*, 268(8), 2512–2519. doi:10.1046/j.1432-1327.2001.02140.x

Scarpulla R. C. (2011). Metabolic Control of Mitochondrial Biogenesis Through the PGC-1 Family Regulatory Network. *Biochimica et biophysica acta*, *1813*(7), 1269–1278. doi:10.1016/j.bbamcr.2010.09.019

Scarpulla, R. C. (2008). Transcriptional Paradigms in Mammalian Mitochondrial Biogenesis and Function. *Physiological Reviews*, 88(2), 611–638. doi:10.1152/physrev.00025.2007

Scarpulla, R. C. (2006). Nuclear Control of Respiratory Gene Expression in Mammalian Cells. *Journal of cellular biochemistry*, 97(4), 673–683. doi:10.1002/jcb.20743

Shimazu, T., Hirschey, M. D., Newman, J., He, W., Shirakawa, K., Le Moan, N., Grueter, C.A., Lim, H., Saunders, L.R., Stevens, R.D., Newgard, C.B., Farese, R.V., de Cabo, R., Ulrich, S., Akassoglou, K., & Verdin, E. (2013). Suppression of Oxidative Stress by β-hydroxybutyrate, an Endogenous Histone Deacetylase Inhibitor. *Science (New York, N.Y.)*, *339*(6116), 211–214. doi:10.1126/science.1227166

Shukla, S. K., Gebregiworgis, T., Purohit, V., Chaika, N. V., Gunda, V., Radhakrishnan, P., Mehla, K., Pipinos, I.I., Powers, R., Yu, F., & Singh, P. K. (2014). Metabolic Reprogramming Induced by Ketone Bodies Diminishes Pancreatic Cancer Cachexia. *Cancer & metabolism*, 2: 18. doi:10.1186/2049-3002-2-18

Stallons, L. J., Funk, J. A., & Schnellmann, R. G. (2013). Mitochondrial Homeostasis in Acute Organ Failure. *Current Pathobiology Reports*, 1(3), 10.1007/s40139-013-0023-x. doi:10.1007/s40139-013-0023-x

Steinmetz, K. L., & Spack, E. G. (2009). The Basics of Preclinical Drug Development for Neurodegenerative Disease Indications. *BMC neurology*, 9 Suppl 1(Suppl 1), S2. doi:10.1186/1471-2377-9-S1-S2

Usenik, A., & Legiša, M. (2010). Evolution of Allosteric Citrate Binding Sites on 6-Phosphofructo-1-kinase. *PloS one*, 5(11), e15447. doi:10.1371/journal.pone.0015447

Wardell, S. E., Ilkayeva, O. R., Wieman, H. L., Frigo, D. E., Rathmell, J. C., Newgard, C. B., & McDonnell, D. P. (2009). Glucose Metabolism as a Target of Histone Deacetylase Inhibitors. *Molecular endocrinology (Baltimore, Md.)*, 23(3), 388–401. doi:10.1210/me.2008-0179

Weidemann, M. J., & Krebs, H. A. (1969). The Fuel of Respiration of Rat Kidney Cortex. *The Biochemical journal*, 112(2), 149–166. doi:10.1042/bj1120149

Will, Y., & Dykens, J. (2007). The Significance of Mitochondrial Toxicity Testing in Drug Development. *Drug discovery today*, 12(17-18), 777-785. doi.org/10.1016/j.drudis.2007.07.013

Will, Y., & Dykens, J. (2014). Mitochondrial Toxicity Assessment in Industry – A Decade of Technology Development and Insight. *Expert opinion on drug metabolism & toxicology*, 10(8), 1061–1067. doi:10.1517/17425255.2014.939628

Wills, L. P. (2017). The use of High-Throughput Screening Techniques to Evaluate Mitochondrial Toxicity. *Toxicology*, 391, 34–41. doi:10.1016/j.tox.2017.07.020

Wills, L. P., Beeson, G. C., Hoover, D. B., Schnellmann, R. G., & Beeson, C. C. (2015). Assessment of ToxCast phase II for Mitochondrial Liabilities Using a High-Throughput Respirometric Assay. *Toxicological sciences*, 146(2), 226–234. doi: 10.1093/toxsci/kfv085

VITA

Name	Trudi Denoon
Baccalaureate Degree	Bachelor of Science
	St. John's University, New York
Date Graduated	January 2008
Master's Degree	Master of Science
	St. John's University, New York
Date Graduated	January 2012
Doctoral Degree	Doctor of Philosophy
	St. John's University, New York
Date Graduated	January 2020